

## $\pi$ - and $K$ -meson Bethe-Salpeter amplitudes

Pieter Maris and Craig D. Roberts

*Physics Division, Building 203, Argonne National Laboratory, Argonne, Illinois 60439-4843*

(Received 18 August 1997)

Independent of assumptions about the form of the quark-quark scattering kernel  $K$ , we derive the explicit relation between the flavor-nonsinglet pseudoscalar-meson Bethe-Salpeter amplitude  $\Gamma_H$  and the dressed-quark propagator in the chiral limit. In addition to a term proportional to  $\gamma_5$ ,  $\Gamma_H$  necessarily contains qualitatively and quantitatively important terms proportional to  $\gamma_5 \gamma \cdot P$  and  $\gamma_5 \gamma \cdot k k \cdot P$ , where  $P$  is the total momentum of the bound state. The axial-vector vertex contains a bound state pole described by  $\Gamma_H$ , whose residue is the leptonic decay constant for the bound state. The pseudoscalar vertex also contains such a bound state pole and, in the chiral limit, the residue of this pole is related to the vacuum quark condensate. The axial-vector Ward-Takahashi identity relates these pole residues, with the Gell-Mann–Oakes–Renner relation a corollary of this identity. The dominant ultraviolet asymptotic behavior of the scalar functions in the meson Bethe-Salpeter amplitude is fully determined by the behavior of the chiral limit quark mass function, and is characteristic of the QCD renormalization group. The rainbow-ladder *Ansatz* for  $K$ , with a simple model for the dressed-quark-quark interaction, is used to illustrate and elucidate these general results. The model preserves the one-loop renormalization group structure of QCD. The numerical studies also provide a means of exploring procedures for solving the Bethe-Salpeter equation without a three-dimensional reduction. [S0556-2813(97)04112-5]

PACS number(s): 14.40.Aq, 24.85.+p, 11.10.St, 12.38.Lg

### I. INTRODUCTION

$\pi$  and  $K$  mesons are the lightest hadrons and hence they play a significant role in the phenomenology of low-to-intermediate energy nuclear physics as mediators of the long-range part of the hadron-hadron interaction. They are easily produced in electron-nucleon and nucleon-nucleon collisions and therefore provide an ideal means of exploring models of hadronic structure and subnucleonic degrees of freedom in nuclei. As mesons, the simple quark-antiquark valence-quark content of the  $\pi$  and  $K$  makes them the simplest light-quark systems one can study as strong interaction bound states, and this is a necessary step in developing a detailed understanding of their properties and interactions in terms of the elementary degrees of freedom in QCD.

Mesonic bound states are described by the homogeneous Bethe-Salpeter equation (BSE), which is one of the Dyson-Schwinger equations [1] (DSE's) characterizing QCD. The homogeneous BSE is an eigenvalue problem whose eigenvalue is  $P^2$ , the square of the bound state mass, and whose eigenvector is the bound state amplitude (fully amputated, quark-antiquark-meson vertex). This bound state, or Bethe-Salpeter, amplitude is a crucial element in the calculation of production and scattering processes involving mesons, as illustrated in Refs. [1–3]. The BSE is familiar in the study of scattering and binding in two-nucleon systems, and it is often illustrated, and its features explored, via the problem of two elementary scalars interacting via the exchange of a different elementary scalar [4]. There have been many applications to the strong interaction meson spectrum, with recent, extensive studies in this general framework being those of Refs. [6–8], which also cite related research.

Bethe-Salpeter equation studies can be characterized by their treatment of the quark-antiquark scattering kernel  $K(q, k; P)$ , a concrete calculation being specified by a trun-

cation of the skeleton expansion for  $K$ . This kernel also appears implicitly in the DSE for the dressed-quark propagator (the QCD “gap equation”) via the dressed-quark-gluon vertex  $\Gamma_v^a(q, p)$ . In studies of the spectrum and interactions of the bound states of light quarks, where dynamical chiral symmetry breaking (DCSB) and Goldstone's theorem are particularly important, it is crucial to ensure that  $K$  and  $\Gamma_v^a$  are “mutually consistent,” by which we mean that they must be such as to guarantee the preservation of the axial-vector Ward-Takahashi identity [9]. Otherwise, as discussed and exemplified in Refs. [7,8,10], a qualitatively correct description of the light-quark meson spectrum is not possible; i.e., “fine-tuning” is necessary to properly describe the *theoretical ideal* of the chiral limit, and the observational fact that the pion is so much lighter than the characteristic hadronic scale:  $m_\rho/2 \approx m_N/3 \doteq M_q$ , the constituent quark mass, but  $m_\pi/2 \approx 0.2M_q$ .

The rainbow-ladder truncation of the quark-DSE and meson-BSE, without a three-dimensional reduction, is a specification of  $\Gamma_v^a$  and  $K$  that ensures the preservation of the axial-vector Ward-Takahashi identity. It is fully specified by an *Ansatz* for the dressed-quark-quark interaction and allows a qualitatively and quantitatively good description of flavor-nonsinglet pseudoscalar, vector, and axial vector mesons without fine-tuning, even in very simple models [11]. As such it is a phenomenologically efficacious tool in this sector.

The fact that it describes the flavor-singlet pseudoscalar and scalar mesons poorly is not often mentioned. However, this defect is not crucial now that its source has been identified and understood [12,13]. Employing a straightforward and systematic procedure for extending the rainbow-ladder truncation, a procedure that preserves the axial-vector Ward-Takahashi identity at every order, allows one to analyze the attractive and repulsive terms order by order beyond ladder

truncation in the BSE. One finds, for example, that in the flavor-nonsinglet pseudoscalar channel the repulsive terms are approximately canceled by attractive terms that arise at the same order, which explains why the ladder truncation provides a good approximation in this channel. This is not the case in the scalar channel where higher-order terms do not cancel in a like manner but lead to a net repulsive effect, whose magnitude cannot be estimated *a priori* but which entails that the ladder truncation provides a poor approximation. In the flavor-singlet pseudoscalar channel, timelike gluon exchange diagrams arise when one improves upon the ladder truncation and these provide a plausible mechanism for splitting the flavor-singlet and flavor-nonsinglet mesons, i.e., for generating a significant  $\eta$ - $\eta'$  mass splitting [14]. These observations illustrate and emphasize that the rainbow-ladder truncation can lead to qualitatively and quantitatively reliable conclusions if used judiciously.

Our goal herein is to provide a concrete illustration of the general results of Ref. [9], i.e., of the importance, feasibility, and essential consequences of preserving the axial-vector Ward-Takahashi identity in BSE studies of quark-antiquark bound states, and the extension of these results to  $SU(N_f \geq 3)$ . We employ a renormalizable DSE model of QCD that preserves the one-loop renormalization characteristics of the dressed-quark and -gluon propagators and the quark-gluon vertex. This allows an explicit demonstration of the renormalization group flow of the vacuum quark condensate, for example, and renormalization point independence of physical observables in this framework. We concentrate on the  $\pi$  and  $K$  mesons since this subsystem has all the complexity necessary for a complete discussion of the features we wish to elucidate.

In Sec. II we describe the DSE for the renormalized dressed-quark propagator, this propagator being a critical element in the construction of the kernel in the BSE for meson bound states. We discuss this BSE in Sec. III, along with the constraints entailed by preserving the axial-vector Ward-Takahashi identity. In Sec. IV we report a model study of the quark DSE and meson BSE, and a range of  $\pi$ - and  $K$ -meson observables, illustrating the model-independent results derived in the preceding sections. We summarize and conclude in Sec. V.

## II. QUARK DYSON-SCHWINGER EQUATION

In a Euclidean space formulation, with  $\{\gamma_\mu, \gamma_\nu\} = 2\delta_{\mu\nu}$ ,  $\gamma_\mu^\dagger = \gamma_\mu$ , and  $a \cdot b = \sum_{i=1}^4 a_i b_i$ , the DSE for the renormalized dressed-quark propagator is

$$S(p)^{-1} = Z_2(i\gamma \cdot p + m_{\text{bm}}) + Z_1 \int_q^\Lambda g^2 D_{\mu\nu}(p-q) \frac{\lambda^a}{2} \gamma_\mu S(q) \times \Gamma_\nu^a(q,p), \quad (1)$$

where  $D_{\mu\nu}(k)$  is the renormalized dressed-gluon propagator,  $\Gamma_\nu^a(q;p)$  is the renormalized dressed-quark-gluon vertex,  $m_{\text{bm}}$  is the  $\Lambda$ -dependent current-quark bare mass that appears in the Lagrangian, and  $\int_q^\Lambda \doteq \int^\Lambda d^4q / (2\pi)^4$  represents mnemonically a *translationally invariant* regularization of the integral, with  $\Lambda$  the regularization mass scale. The final stage of any calculation is to remove the regularization by taking

the limit  $\Lambda \rightarrow \infty$ . The quark-gluon-vertex and quark wave function renormalization constants  $Z_1(\mu^2, \Lambda^2)$  and  $Z_2(\mu^2, \Lambda^2)$ , respectively, depend on the renormalization point and the regularization mass scale, as does the mass renormalization constant  $Z_m(\mu^2, \Lambda^2) \doteq Z_2(\mu^2, \Lambda^2)^{-1} Z_4(\mu^2, \Lambda^2)$ . In Eq. (1),  $S$ ,  $\Gamma_\mu^a$ , and  $m_{\text{bm}}$  depend on the quark flavor, although we have not indicated this explicitly. However, in our analysis we assume, and employ, a flavor-independent renormalization scheme and hence all the renormalization constants are flavor independent.

### A. General remarks about renormalization

#### 1. Dressed-quark propagator

The solution of Eq. (1) has the general form

$$S(p)^{-1} = i\gamma \cdot p A(p^2, \mu^2) + B(p^2, \mu^2) = \frac{1}{Z(p^2, \mu^2)} [i\gamma \cdot p + M(p^2, \mu^2)], \quad (2)$$

renormalized such that, at some large<sup>1</sup> spacelike  $\mu^2$ ,

$$S(p)^{-1}|_{p^2=\mu^2} = i\gamma \cdot p + m(\mu), \quad (3)$$

where  $m(\mu)$  is the renormalized quark mass at the scale  $\mu$ . In the presence of an explicit, chiral-symmetry-breaking, current-quark mass one has  $Z_4 m(\mu) = Z_2 m_{\text{bm}}$ , neglecting  $O(1/\mu^2)$  corrections associated with dynamical chiral symmetry breaking that are intrinsically nonperturbative in origin.

Multiplicative renormalizability in QCD entails that

$$\frac{A(p^2, \mu^2)}{A(p^2, \bar{\mu}^2)} = \frac{Z_2(\mu^2, \Lambda^2)}{Z_2(\bar{\mu}^2, \Lambda^2)} = A(\bar{\mu}^2, \mu^2) = \frac{1}{A(\mu^2, \bar{\mu}^2)}. \quad (4)$$

Such relations can be used as constraints on model studies of Eq. (1). Explicitly, at one-loop order in perturbation theory,

$$Z_2(\mu^2, \Lambda^2) = \left[ \frac{\alpha(\Lambda^2)}{\alpha(\mu^2)} \right]^{-\gamma_F/\beta_1}, \quad (5)$$

where  $\gamma_F = \frac{2}{3}\xi$  and  $\beta_1 = N_f/3 - 11/2$ , with  $\xi$  the gauge parameter and  $N_f$  the number of active quark flavors. At this order,

$$\alpha(Q^2) = \frac{\pi}{-\frac{1}{2}\beta_1 \ln[Q^2/\Lambda_{\text{QCD}}^2]}. \quad (6)$$

Clearly, at one loop in Landau gauge ( $\xi=0$ ),  $A(p^2, \mu^2) \equiv 1$ , and a deviation from this result in a solution of Eq. (1) is a

<sup>1</sup>Herein, by ‘‘large’’ we mean  $\mu^2$  very much greater than the renormalization-group-invariant current-quark mass for the  $s$  quark so as to ensure that, in our model calculations, the renormalization constants are flavor independent to better than 1%. It is possible to employ a modified subtraction scheme in which the renormalization constants are exactly flavor independent; however, it does not quantitatively affect our results and hence is an unnecessary complication [15].

higher-loop effect. Such effects are always present in the self-consistent solution of Eq. (1).

The ratio  $M(p^2, \mu^2) = B(p^2, \mu^2)/A(p^2, \mu^2)$  is independent of the renormalization point in perturbation theory; i.e., with  $\mu \neq \bar{\mu}$ ,

$$M(p^2, \mu^2) = M(p^2, \bar{\mu}^2) \doteq M(p^2), \quad \forall p^2. \quad (7)$$

At one-loop order,

$$m(\mu) \doteq M(\mu^2) = \frac{\hat{m}}{(\frac{1}{2} \ln[\mu^2/\Lambda_{\text{QCD}}^2])^{\gamma_m}}, \quad (8)$$

where  $\hat{m}$  is a renormalization-point-independent current-quark mass,  $\gamma_m = 12/(33 - 2N_f)$  is the anomalous dimension at this order, and

$$Z_m(\mu^2, \Lambda^2) = \left[ \frac{\alpha(\Lambda^2)}{\alpha(\mu^2)} \right]^{\gamma_m}. \quad (9)$$

In QCD,  $\gamma_m$  is independent of the gauge parameter to all orders in perturbation theory and the chiral limit is defined by  $\hat{m} = 0$ . Dynamical chiral symmetry breaking is manifest when, for  $\hat{m} = 0$ , one obtains  $m(\mu) \sim \mathcal{O}(1/\mu^2) \neq 0$  in solving Eq. (1), which is impossible at any finite order in perturbation theory.<sup>2</sup> This is discussed and illustrated in Sec. IV A.

### 2. Dressed-gluon propagator

In a general covariant gauge the renormalized dressed-gluon propagator in Eq. (1) has the general form

$$D_{\mu\nu}(k) = \left( \delta_{\mu\nu} - \frac{k_\mu k_\nu}{k^2} \right) \frac{d(k^2, \mu^2)}{k^2} + \xi \frac{k_\mu k_\nu}{k^4}, \quad (10)$$

where  $d(k^2, \mu^2) = 1/[1 + \Pi(k^2, \mu^2)]$ , with  $\Pi(k^2, \mu^2)$  the renormalized gluon vacuum polarization. The fact that the longitudinal ( $\xi$ -dependent) part of  $D_{\mu\nu}(k)$  is not modified by interactions is the result of a Slavnov-Taylor identity in QCD:  $k_\mu D_{\mu\nu}(k) = \xi k_\nu/k^2$ . We note that Landau gauge is a fixed point of the renormalization group; i.e., in Landau gauge the renormalization-group-invariant gauge parameter is zero to all orders in perturbation theory, and hence we employ this gauge in all numerical studies herein.

Multiplicative renormalizability entails that

$$\frac{d(k^2, \mu^2)}{d(k^2, \bar{\mu}^2)} = \frac{Z_3(\bar{\mu}^2, \Lambda^2)}{Z_3(\mu^2, \Lambda^2)} = d(\mu^2, \bar{\mu}^2) = \frac{1}{d(\bar{\mu}^2, \mu^2)}. \quad (11)$$

At one-loop order in perturbation theory,

<sup>2</sup>The arguments presented herein cannot be applied in a straightforward fashion to models whose ultraviolet behavior is that of quenched QED<sub>4</sub>, such as Ref. [16], where the chiral limit cannot be defined in this way. The difficulties encountered in such cases are illustrated in Ref. [17].

$$Z_3(\mu^2, \Lambda^2) = \left[ \frac{\alpha(\Lambda^2)}{\alpha(\mu^2)} \right]^{-\gamma_1/\beta_1}, \quad (12)$$

where  $\gamma_1 = \frac{1}{3}N_f - \frac{1}{4}(13 - 3\xi)$ .

### 3. Dressed-quark-gluon vertex

The renormalized dressed-quark-gluon vertex in Eq. (1) is of the form

$$\Gamma_\nu^a(k, p) = \frac{\lambda^a}{2} \Gamma_\nu(k, p). \quad (13)$$

As a fully amputated vertex, it is free of kinematic singularities. The general Lorentz structure of  $\Gamma_\nu(k, p)$  is straightforward but lengthy, involving 12 distinct scalar form factors, and here we do not reproduce it fully,

$$\Gamma_\nu(k, p) = \gamma_\nu F_1(k, p, \mu) + \dots, \quad (14)$$

but remark that Ref. [15], pp. 80–83, and Refs. [18,19] provide an elucidation of its structure, evaluation, and properties.

Renormalizability entails that only the form factor  $F_1$ , associated with the  $\gamma_\nu$  tensor, is ultraviolet divergent. By convention and defining  $f_1(k^2, \mu^2) \doteq F_1(k, -k, \mu)$ ,  $\Gamma_\nu(k, p)$  is renormalized such that, at some large spacelike  $\mu^2$ ,

$$f_1(\mu^2, \mu^2) = 1. \quad (15)$$

Since the renormalization is multiplicative, one has

$$\frac{f_1(k^2, \mu^2)}{f_1(k^2, \bar{\mu}^2)} = \frac{Z_1(\mu^2, \Lambda^2)}{Z_1(\bar{\mu}^2, \Lambda^2)} = f_1(\bar{\mu}^2, \mu^2) = \frac{1}{f_1(\mu^2, \bar{\mu}^2)}. \quad (16)$$

At one loop in perturbation theory the vertex renormalization constant is

$$Z_1(\mu^2, \Lambda^2) = \left[ \frac{\alpha(\Lambda^2)}{\alpha(\mu^2)} \right]^{-\gamma_\Gamma/\beta_1}, \quad (17)$$

where  $\gamma_\Gamma = \frac{1}{2}[\frac{3}{4}(3 + \xi) + \frac{4}{3}\xi]$ .

## B. Model for the quark DSE

In order to exemplify the results of Ref. [9], which we reiterate and generalize in Sec. III A, we must know the form of  $D_{\mu\nu}(k)$  and  $\Gamma_\nu(k, p)$ , not only in the ultraviolet where perturbation theory is applicable, but also in the infrared, where perturbation theory fails and lattice simulations are affected by finite-volume artifacts.  $D_{\mu\nu}(k)$  and  $\Gamma_\nu(k, p)$  satisfy DSE's. However, studies of these equations in QCD are rudimentary and are presently best used only to suggest qualitatively reliable *Ansätze* for these Schwinger functions. That is why all quantitative studies of the quark DSE to date have employed model forms of  $D_{\mu\nu}(k)$  and  $\Gamma_\nu(k, p)$ .

### 1. Abelian approximation

To introduce one commonly used pair of *Ansätze*, we use Eqs. (5), (12), and (17) and observe that

$$\frac{2\gamma_F}{\beta_1} + \frac{\gamma_1}{\beta_1} - \frac{2\gamma_\Gamma}{\beta_1} = 1. \quad (18)$$

Hence, on the kinematic domain for which  $Q^2 \doteq (p-q)^2 \sim p^2 \sim q^2$  is large and spacelike, the renormalized dressed-ladder kernel in the Bethe-Salpeter equation for the (fully amputated) Bethe-Salpeter amplitude behaves as follows:

$$\begin{aligned} & g^2(\mu^2)D_{\mu\nu}(p-q) \\ & \times [\Gamma_\mu^a(p_+, q_+)S(q_+)] \times [S(q_-)\Gamma_\nu^a(q_-, p_-)] \\ & = 4\pi\alpha(Q^2)D_{\mu\nu}^{\text{free}}(p-q) \left[ \frac{\lambda^a}{2} \gamma_\mu S^{\text{free}}(q_+) \right] \\ & \times \left[ S^{\text{free}}(q_-) \frac{\lambda^a}{2} \gamma_\nu \right], \end{aligned} \quad (19)$$

where  $P$  is the total quark-antiquark momentum,  $p_+ \doteq p + \eta_p P$ , and  $p_- \doteq p - (1 - \eta_p)P$  [see Eq. (25)]. This observation, and the intimate relation between the kernel of the pseudoscalar BSE and the integrand in Eq. (1) [12], provides a means of understanding the origin of an often used *Ansatz* for  $D_{\mu\nu}(k)$ , i.e., in Landau gauge, making the replacement

$$g^2 D_{\mu\nu}(k) \rightarrow 4\pi\alpha(k^2) D_{\mu\nu}^{\text{free}}(k) \quad (20)$$

in Eq. (1), and using the ‘‘rainbow approximation’’

$$\Gamma_\nu(q, p) = \gamma_\nu. \quad (21)$$

The *Ansatz* expressed in Eq. (20) is often described as the ‘‘Abelian approximation’’ because the left- and right-hand sides are *equal* in QED. In QCD, equality between the two sides of Eq. (20) cannot be obtained easily by a selective resummation of diagrams. As reviewed in Ref. [1], Eqs. (5.1)–(5.8), it can only be achieved by enforcing equality between the renormalization constants for the ghost-gluon vertex and ghost wave function:  $\bar{Z}_1 = \bar{Z}_3$ .

A mutually consistent constraint, which follows from  $\bar{Z}_1 = \bar{Z}_3$  at a formal level, is to enforce the Abelian Ward identity  $Z_1 = Z_2$ . At one loop this corresponds to neglecting the contribution of the three-gluon vertex to  $\Gamma_\nu$ , in which case  $\gamma_\Gamma \rightarrow \frac{2}{3}\xi = \gamma_F$ . This additional constraint provides the basis for extensions of Eq. (21), i.e., using *Ansätze* for  $\Gamma_\nu$  that are consistent with the vector Ward-Takahashi identity in QED [20], such as Refs. [21–23].

The combination of Abelian and rainbow approximations (with  $Z_1 = 1 = Z_2$ ) yields a mass function  $M(p^2)$ , with the ‘‘correct’’ one-loop anomalous dimension, i.e.,  $\gamma_m$  in Eq. (8) in the case of explicit chiral symmetry breaking or  $(1 - \gamma_m)$  in its absence [24]. However, other often used *Ansätze* for  $\Gamma_\nu$  [18,25] yield different and incorrect anomalous dimensions for  $M(p^2)$  [26]. This illustrates and emphasizes that the anomalous dimension of the solution of Eq. (1) is sensitive to the details of the asymptotic behavior of the *Ansätze* for the elements in the integrand. One role of the multiplicative renormalization constant  $Z_1$  is to compensate for this.

## 2. Model for $g^2 D_{\mu\nu}(p-q)\Gamma_\nu(q, p)$

Herein we employ a model for the kernel of Eq. (1) based on the Abelian approximation:

$$\begin{aligned} & Z_1 \int_q^\Lambda g^2 D_{\mu\nu}(p-q) \frac{\lambda^a}{2} \gamma_\mu S(q) \Gamma_\nu^a(q, p) \\ & \rightarrow \int_q^\Lambda \mathcal{G}((p-q)^2) D_{\mu\nu}^{\text{free}}(p-q) \frac{\lambda^a}{2} \gamma_\mu S(q) \frac{\lambda^a}{2} \gamma_\nu, \end{aligned} \quad (22)$$

with the specification of the model complete once a form is chosen for the ‘‘effective coupling’’  $\mathcal{G}(k^2)$ .

One consideration underlying this *Ansatz* is that we wish to study subtractive renormalization in a DSE model of QCD and it is not possible to determine  $Z_1$  without analyzing the DSE for the dressed-quark-gluon vertex, a problem we postpone. Instead we explored various *Ansätze* for  $\Gamma_\nu$  and found that, with  $\mathcal{G}(k^2) = 4\pi\alpha(k^2)$  for large  $k^2$ , there was always at least one *Ansatz* for  $Z_1$  that led to the correct anomalous dimension for  $M(p^2)$ . This interplay between the the renormalization constant and the integral is manifest in QCD and Eq. (22) is a simple means of implementing it.

In choosing a form for  $\mathcal{G}(k^2)$  we noted that the behavior of  $\alpha(k^2)$  in the ultraviolet, i.e., for  $k^2 > 1-2 \text{ GeV}^2$ , is well described by perturbation theory. Constraints on the form of  $\mathcal{G}(k^2)$  in the infrared come from the DSE satisfied by the dressed-gluon propagator  $D_{\mu\nu}(k)$ . As summarized succinctly in Refs. [13,27], qualitatively reliable studies of this equation indicate that the dressed-quark-quark interaction is significantly enhanced in the infrared such that on this domain it is well represented by an integrable singularity [28]. Combining these observations with Eqs. (18)–(20), which illustrate the necessary interplay between the anomalous dimensions of each term in the integrand of Eq. (1), motivates the *Ansatz*

$$\begin{aligned} \frac{\mathcal{G}(k^2)}{k^2} &= 8\pi^4 D \delta^4(k) + \frac{4\pi^2}{\omega^6} D k^2 e^{-k^2/\omega^2} \\ &+ 4\pi \frac{\gamma_m \pi}{\frac{1}{2} \ln[\tau + (1 + k^2/\Lambda_{\text{QCD}}^2)^2]} \mathcal{F}(k^2), \end{aligned} \quad (23)$$

with  $\mathcal{F}(k^2) = \{1 - \exp(-k^2/[4m_t^2])\}/k^2$  and  $\tau = e^2 - 1$ . (We use  $N_f = 4$  and  $\Lambda_{\text{QCD}}^{N_f=4} = 0.234 \text{ GeV}$  in our numerical studies.) This is a simple modification of the form used in Ref. [16], one which preserves the one-loop renormalization group behavior of QCD in the quark DSE.

The qualitative features of Eq. (23) are clear. The first term is an integrable infrared singularity [29] and the second is a finite-width approximation to  $\delta^4(k)$ , normalized such that it has the same  $\int d^4k$  as the first term. In this way we split the infrared singularity into the sum of a zero-width and a finite-width piece. The last term in Eq. (23) is proportional to  $\alpha(k^2)/k^2$  at large spacelike  $k^2$  and has no singularity on the real- $k^2$  axis.

There are ostensibly three parameters in Eq. (23):  $D$ ,  $\omega$ , and  $m_t$  ( $D = 2\gamma_m m_t^2$  in Ref. [16]). However, in our numerical studies, using a renormalization point  $\mu = 19 \text{ GeV}$ , which is large enough to be in the perturbative domain, we fixed  $\omega = 0.3 \text{ GeV}$  [ $= 1/(0.66 \text{ fm})$ ] and  $m_t = 0.5 \text{ GeV}$  [ $= 1/(0.39 \text{ fm})$ ], and only varied  $D$  and the renormalized  $u/d$ - and

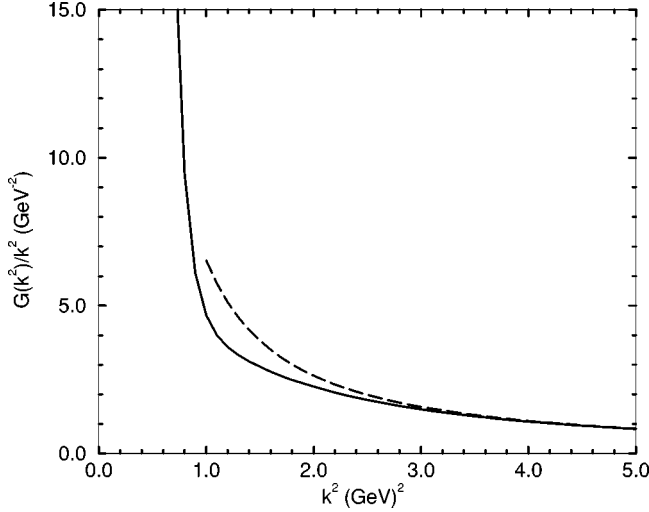


FIG. 1. A comparison of  $\mathcal{G}(k^2)/k^2$  in Eq. (23) obtained using the best fit parameters of Eq. (24) (solid line), with  $4\pi\alpha(k^2)/k^2$  in Eq. (6) (dashed line). The obvious infrared enhancement is qualitatively and semiquantitatively in agreement with that inferred in the gluon DSE studies of Ref. [28].

$s$ -current-quark masses in order to obtain a good description of low-energy  $\pi$ - and  $K$ -meson properties. As shown below, this is achieved with

$$D = 0.781 \text{ GeV}^2, \quad m_{u/d}(\mu) = 3.74 \text{ MeV},$$

$$m_s(\mu) = 82.5 \text{ MeV}. \quad (24)$$

(We do not consider isospin-breaking effects herein.) We chose the quoted values of  $\omega$  and  $m_t$  primarily so as to ensure that  $\mathcal{G}(k^2) \approx 4\pi\alpha(k^2)$  for  $k^2 > 2 \text{ GeV}^2$ , as illustrated in Fig. 1. This is sufficient for our present illustrative study, just as the form in Ref. [16] was sufficient therein. However, increasing sophistication and/or an exploration of a broader range of observables is likely to require a more careful treatment of this or other parametric forms.

Evolved according to Eq. (8), postponing until Sec. IV A the discussion of whether this formula is appropriate, the ‘‘best fit’’ mass values in Eq. (24) correspond to  $m_{u/d}^{1 \text{ GeV}} = 6.4 \text{ MeV}$  and  $m_s^{1 \text{ GeV}} = 140 \text{ MeV}$ . The ‘‘best fit’’ values are sensitive to the behavior of  $\mathcal{G}(k^2)$  for  $k^2 \sim 1-2 \text{ GeV}^2$ , which can be illustrated by their dependence on  $\omega$ : Increasing  $\omega \rightarrow 1.5\omega$ , while maintaining a good fit to  $\pi$ - and  $K$ -meson observables, requires a  $\sim 10\%$  reduction in the value of these masses. With minor modifications of our parametrization we can satisfy our phenomenological constraints using current-quark masses that are a factor of  $\sim 1.5-2$ , smaller, as canvassed in Ref. [30]. We would have to apply tighter constraints in our phenomenological application to make a statement about the current-quark masses of light quarks that is more accurate than this. These considerations do not affect the ratio of our fitted current-quark mass values,  $m_s(\mu)/m_{u/d}(\mu) = 22.0$ , which is consistent with Refs. [6,11] and the discussion of Ref. [30].

### III. PION AND KAON BETHE-SALPETER EQUATIONS

The renormalized, homogeneous, pseudoscalar Bethe-Salpeter equation is

$$[\Gamma_H(k;P)]_{tu} = \int_q^\Lambda [\chi_H(q;P)]_{sr} K_{tu}^{rs}(q,k;P), \quad (25)$$

where  $H = \pi$  or  $K$  specifies the flavor-matrix structure of the amplitude;  $\chi_H(q;P) \doteq \mathcal{S}(q_+) \Gamma_H(q;P) \mathcal{S}(q_-)$ , with  $\mathcal{S}(q) = \text{diag}(S_u(q), S_d(q), S_s(q))$ ;  $q_+ = q + \eta_P P$ ,  $q_- = q - (1 - \eta_P)P$ , with  $P$  the total momentum of the bound state; and  $r, \dots, u$  represent color-, Dirac- and flavor-matrix indices.

In Eq. (25),  $K_{tu}^{rs}(q,k;P)$  is the renormalized, fully-amputated quark-antiquark scattering kernel, which also appears implicitly in Eq. (1) because it is the kernel in the inhomogeneous integral equation satisfied by  $\Gamma_v(q;p)$ .  $K_{tu}^{rs}(q,k;P)$  is a four-point Schwinger function obtained as the sum of a countable infinity of skeleton diagrams. It is two-particle irreducible, with respect to the quark-antiquark pair of lines and does not contain quark-antiquark to single gauge-boson annihilation diagrams, such as would describe the leptonic decay of a pseudoscalar meson.<sup>3</sup> The complexity of  $K_{tu}^{rs}(q,k;P)$  is one reason why quantitative studies of the quark DSE currently employ *Ansätze* for  $D_{\mu\nu}(k)$  and  $\Gamma_v(k,p)$ . As illustrated by Ref. [9], however, the complexity of  $K_{tu}^{rs}(q,k;P)$  does not prevent one from analyzing aspects of QCD in a model-independent manner and proving general results that provide useful constraints on model studies of QCD.

Equation (25) is an eigenvalue problem. Solutions exist only for particular, separated values of  $P^2$ , and the eigenvector associated with each eigenvalue, the Bethe-Salpeter amplitude (BSA)  $\Gamma_H(k;P)$ , is the one-particle-irreducible, fully amputated quark-meson vertex. In the flavor-octet channels the solutions with the lowest eigenvalues are the  $\pi$  and  $K$  mesons.<sup>4</sup> The solution of Eq. (25) has the general form [32]

$$\Gamma_H(k;P) = T^H \gamma_5 [iE_H(k;P) + \gamma \cdot P F_H(k;P) + \gamma \cdot k k \cdot P G_H(k;P) + \sigma_{\mu\nu} k_\mu P_\nu H_H(k;P)], \quad (26)$$

where for bound states of constituents with equal current-quark masses the scalar functions  $E$ ,  $F$ ,  $G$ , and  $H$  are even under  $k \cdot P \rightarrow -k \cdot P$  and, for example,  $T^{K^+} = \frac{1}{2}(\lambda^4 + i\lambda^5)$ , with  $\{\lambda^j, j=1, \dots, 8\}$  the SU(3)-flavor Gell-Mann matrices. The requirement that the bound state contribution to the fully amputated quark-antiquark scattering amplitude,  $M = K + K(SS)K + \dots$ , have unit residue leads to the canonical normalization condition for the BSA:

$$2P_\mu = \int_q^\Lambda \left\{ \text{tr} \left[ \bar{\Gamma}_H(q; -P) \frac{\partial \mathcal{S}(q_+)}{\partial P_\mu} \Gamma_H(q; P) \mathcal{S}(q_-) \right] + \text{tr} \left[ \bar{\Gamma}_H(q; -P) \mathcal{S}(q_+) \Gamma_H(q; P) \frac{\partial \mathcal{S}(q_-)}{\partial P_\mu} \right] \right\}$$

<sup>3</sup>A connection between the fully amputated quark-antiquark scattering amplitude;  $M = K + K(SS)K + \dots$ , and the Wilson loop is discussed in Ref. [31].

<sup>4</sup>We do not consider the  $\eta$  meson because of its mixing with the  $\eta'$ , which cannot be described in ladder approximation [11,12], the truncation of the BSE employed in Sec III B.

$$+ \int_q^\Lambda \int_k^\Lambda [\bar{\chi}_H(q; -P)]_{sr} \frac{\partial K_{tu}^{rs}(q, k; P)}{\partial P_\mu} [\chi_H(k; P)]_{ut}, \quad (27)$$

where  $\bar{\Gamma}_H(k, -P)^\dagger = C^{-1} \Gamma_H(-k, -P) C$ , with  $C = \gamma_2 \gamma_4$ , the charge conjugation matrix, and  $X^\dagger$  denoting the matrix transpose of  $X$ .

In Eq. (25),  $E_H(k; P) \neq 0$  acts as a ‘‘source’’ in the equations for  $F_H(k; P)$ ,  $G_H(k; P)$ , and  $H_H(k; P)$  so that, in general, these subleading Dirac components of  $\Gamma_H(k; P)$  are nonzero.

### A. Chiral symmetry

In studies of flavor-octet pseudoscalar mesons a good understanding of chiral symmetry, and its explicit and dynamical breaking, is crucial. These features are expressed in the renormalized axial-vector Ward-Takahashi identity (AV WTI)

$$\begin{aligned} -i P_\mu \Gamma_{5\mu}^H(k; P) &= \mathcal{S}^{-1}(k_+) \gamma_5 \frac{T^H}{2} + \gamma_5 \frac{T^H}{2} \mathcal{S}^{-1}(k_-) \\ &\quad - M_{(\mu)} \Gamma_5^H(k; P) - \Gamma_5^H(k; P) M_{(\mu)}, \end{aligned} \quad (28)$$

where  $M_{(\mu)} = \text{diag}(m_u(\mu), m_d(\mu), m_s(\mu))$ ; the renormalized axial-vector vertex is given by

$$\begin{aligned} [\Gamma_{5\mu}^H(k; P)]_{tu} &= Z_2 \left[ \gamma_5 \gamma_\mu \frac{T^H}{2} \right]_{tu} \\ &\quad + \int_q^\Lambda [\chi_{5\mu}^H(q; P)]_{sr} K_{tu}^{rs}(q, k; P), \end{aligned} \quad (29)$$

with  $\chi_{5\mu}^H(q; P) \doteq \mathcal{S}(q_+) \Gamma_{5\mu}^H(q; P) \mathcal{S}(q_-)$ ; and the renormalized pseudoscalar vertex by

$$[\Gamma_5^H(k; P)]_{tu} = Z_4 \left[ \gamma_5 \frac{T^H}{2} \right]_{tu} + \int_q^\Lambda [\chi_5^H(q; P)]_{sr} K_{tu}^{rs}(q, k; P), \quad (30)$$

with  $\chi_5^H(q; P) \doteq \mathcal{S}(q_+) \Gamma_5^H(q; P) \mathcal{S}(q_-)$ . Multiplicative renormalizability ensures that no new renormalization constants appear in Eqs. (29) and (30) [9,33].

Any study whose goal is a unified understanding of the properties of flavor-octet pseudoscalar mesons and other hadronic bound states must ensure the preservation of the AV WTI, which correlates the axial-vector vertex, pseudoscalar vertex, bound state amplitudes, and quark propagators.

#### 1. Chiral limit

Equation (28) is valid for all values of the renormalization-group-invariant current-quark masses, in particular for the chiral limit when  $M_{(\mu)} \Gamma_5^H(k; P) = \text{diag}(0, 0, 0) = \Gamma_5^H(k; P) M_{(\mu)}$ . In this case the AV WTI is

$$-i P_\mu \Gamma_{5\mu}^H(k; P) = \mathcal{S}^{-1}(k_+) \gamma_5 \frac{T^H}{2} + \gamma_5 \frac{T^H}{2} \mathcal{S}^{-1}(k_-). \quad (31)$$

As a straightforward generalization of Ref. [9], it follows from Eqs. (2) and (31) that in the chiral limit the axial-vector vertex has the form

$$\begin{aligned} \Gamma_{5\mu}^H(k; P) &= \frac{T^H}{2} \gamma_5 [\gamma_\mu F_R(k; P) + \gamma \cdot k k_\mu G_R(k; P) \\ &\quad - \sigma_{\mu\nu} k_\nu H_R(k; P)] + \bar{\Gamma}_{5\mu}^H(k; P) \\ &\quad + f_H \frac{P_\mu}{P^2} \Gamma_H(k; P), \end{aligned} \quad (32)$$

where  $F_R$ ,  $G_R$ ,  $H_R$ , and  $\bar{\Gamma}_{5\mu}^H$  are regular as  $P^2 \rightarrow 0$ ,  $P_\mu \bar{\Gamma}_{5\mu}^H(k; P) \sim O(P^2)$ ,  $\Gamma_H(k; P)$  is the pseudoscalar BSA in Eq. (26), and the residue of the pseudoscalar pole in the axial-vector vertex is  $f_H$ , the leptonic decay constant:

$$f_H P_\mu = Z_2 \int_q^\Lambda \frac{1}{2} \text{tr}[(T^H)^\dagger \gamma_5 \gamma_\mu \mathcal{S}(q_+) \Gamma_H(q; P) \mathcal{S}(q_-)], \quad (33)$$

with the trace over color, Dirac, and flavor indices. In addition the chiral limit AV WTI entails

$$f_H E_H(k; 0) = B(k^2), \quad (34)$$

$$F_R(k; 0) + 2f_H F_H(k; 0) = A(k^2), \quad (35)$$

$$G_R(k; 0) + 2f_H G_H(k; 0) = 2A'(k^2), \quad (36)$$

$$H_R(k; 0) + 2f_H H_H(k; 0) = 0, \quad (37)$$

where  $A(k^2)$  and  $B(k^2)$  are the solutions of Eq. (1) in the chiral limit.

As remarked above, in perturbation theory,  $B(k^2) \equiv 0$  in the chiral limit. The appearance of a  $B(k^2)$ -nonzero solution of Eq. (1) in the chiral limit signals DCSB: One has *dynamically generated* a momentum-dependent quark mass term in the absence of a seed mass. Equations (32) and (34)–(37) show that when chiral symmetry is dynamically broken: (1) the homogeneous, flavor-nonsinglet, pseudoscalar BSE has a massless,  $P^2 = 0$ , solution; (2) the BSA for the massless bound state has a term proportional to  $\gamma_5$  alone, with the momentum dependence of  $E_H(k; 0)$  completely determined by that of the scalar part of the quark self energy, in addition to terms proportional to other pseudoscalar Dirac structures,  $F_H$ ,  $G_H$ , and  $H_H$ , that are nonzero in general; and (3) the axial-vector vertex  $\Gamma_{5\mu}^H(k; P)$  is dominated by the pseudoscalar bound state pole for  $P^2 \approx 0$ . The converse is also true.

The relationship, in the chiral limit, between the normalization of the pseudoscalar BSA and  $f_H$  has often been discussed, for example, Refs. [16,34]. Consider that if one chooses to normalize  $\Gamma_H$  such that  $E_H(0; 0) = B(0)$ , and defines the BSA so normalized as  $\Gamma_H^{NH}(k; P)$ , then the right-hand side of Eq. (27), evaluated with  $\Gamma_H \rightarrow \Gamma_H^{NH}(k; P)$ , is equal to  $2P_\mu N_H^2$ , where  $N_H$  is a dimensioned constant. Using Eqs. (34)–(37) it is clear that, in the chiral limit,

$$N_H = f_H. \quad (38)$$

However, in model studies to date, this result is not obtained *unless* one assumes  $A(k^2) \equiv 1$ . It follows that any kernel which leads, via (1), to  $A(k^2) \equiv 1$  must also yield  $F_H \equiv 0 \equiv G_H \equiv H_H$ , if it preserves the AV WTI. In realistic model studies, where  $A(k^2) \neq 1$ , the difference between the values of  $N_H$  and  $f_H$  is an artifact of neglecting  $F_H$ ,  $G_H$ , and  $H_H$  in Eq. (26) [1].

## 2. Explicit chiral symmetry breaking

Again as a straightforward generalization of Ref. [9], in the presence of explicit chiral symmetry breaking the AV WTI, Eq. (28), entails that both the axial-vector and the pseudoscalar vertices have a pseudoscalar pole, i.e.,

$$\begin{aligned} \Gamma_{5\mu}^H(k;P) &= \frac{T^H}{2} \gamma_5 [\gamma_\mu F_R^H(k;P) + \gamma \cdot k k_\mu G_R^H(k;P) \\ &\quad - \sigma_{\mu\nu} k_\nu H_R^H(k;P)] + \tilde{\Gamma}_{5\mu}^H(k;P) \\ &\quad + f_H \frac{P_\mu}{P^2 + m_H^2} \Gamma_H(k;P), \end{aligned} \quad (39)$$

and

$$\begin{aligned} \Gamma_5^H(k;P) &= \frac{T^H}{2} \gamma_5 [i \mathcal{E}_R^H(k;P) + \gamma \cdot P \mathcal{F}_R^H(k;P) \\ &\quad + \gamma \cdot k k \cdot P \mathcal{G}_R^H(k;P) + \sigma_{\mu\nu} k_\mu P_\nu \mathcal{H}_R^H(k;P)] \\ &\quad + r_H \frac{1}{P^2 + m_H^2} \Gamma_H(k;P), \end{aligned} \quad (40)$$

with  $\mathcal{E}_R^H$ ,  $F_R^H$ ,  $\mathcal{F}_R^H$ ,  $G_R^H$ ,  $\mathcal{G}_R^H$ ,  $H_R^H$ ,  $\mathcal{H}_R^H$ , and  $\tilde{\Gamma}_{5\mu}^H$  regular as  $P^2 \rightarrow -m_H^2$ ;  $P_\mu \tilde{\Gamma}_{5\mu}^H(k;P) \sim O(P^2)$ ; and

$$f_H m_H^2 = r_H \mathcal{M}_H, \quad \mathcal{M}_H \doteq \text{tr}_{\text{flavor}} [M_{(\mu)} \{T^H, (T^H)^\dagger\}], \quad (41)$$

where  $f_H$  is given by Eq. (33), with massive quark propagators in this case, and the residue of the pole in the pseudoscalar vertex is

$$i r_H = Z_4 \int_q^\Lambda \frac{1}{2} \text{tr} [(T^H)^\dagger \gamma_5 \mathcal{S}(q_+) \Gamma_H(q;P) \mathcal{S}(q_-)]. \quad (42)$$

The factor  $Z_4$  on the right-hand side depends on the gauge parameter, the regularization mass scale, and the renormalization point. This dependence is exactly that required to ensure that (1)  $r_H$  is finite in the limit  $\Lambda \rightarrow \infty$ ; (2)  $r_H$  is gauge-parameter independent, and (3) the renormalization point dependence of  $r_H$  is just such as to ensure that the right-hand side of Eq. (41) is renormalization point *independent*. This is obvious at one-loop order, especially in Landau gauge where  $Z_2 \equiv 1$  and hence  $Z_4 = Z_m$ .

In the chiral limit, using Eqs. (26) and (34)–(37), Eq. (42) yields

$$\begin{aligned} r_H^0 &= -\frac{1}{f_H^0} \langle \bar{q} q \rangle_\mu^0, \\ -\langle \bar{q} q \rangle_\mu^0 &\doteq Z_4(\mu^2, \Lambda^2) N_c \int_q^\Lambda \text{tr}_{\text{Dirac}} [\mathcal{S}_{\hat{m}=0}(q)], \end{aligned} \quad (43)$$

where the superscript ‘‘0’’ denotes that the quantity is evaluated in the chiral limit and  $\langle \bar{q} q \rangle_\mu^0$ , as defined here, is the chiral limit *vacuum quark condensate*, which is renormalization point dependent but independent of the gauge parameter and the regularization mass scale. Equation (40) is the statement that *the chiral limit residue of the bound state pole in the flavor-nonsinglet pseudoscalar vertex is  $(-\langle \bar{q} q \rangle_\mu^0)/f_H^0$* . From Eqs. (41) and (43) one obtains immediately

$$f_\pi^2 m_\pi^2 = -[m_u(\mu) + m_d(\mu)] \langle \bar{q} q \rangle_\mu^0 + O(\hat{m}_q^2), \quad (44)$$

$$f_{K^+}^2 m_{K^+}^2 = -[m_u(\mu) + m_s(\mu)] \langle \bar{q} q \rangle_\mu^0 + O(\hat{m}_q^2), \quad (45)$$

which exemplify what is commonly known as the Gell-Mann–Oakes–Renner relation.

We emphasize that the primary result, Eq. (41), of which Eqs. (44) and (45) are corollaries, is valid *independent* of the magnitude of  $\hat{m}_q$ . We can rewrite it in the form

$$f_H^2 m_H^2 = -\langle \bar{q} q \rangle_\mu^H \mathcal{M}_H, \quad (46)$$

where we have introduced the *notation*

$$-\langle \bar{q} q \rangle_\mu^H \doteq f_H r_H \quad (47)$$

in order to highlight the fact that, for nonzero current-quark masses, Eq. (41) *does not* involve a difference of vacuum massive-quark condensates, a phenomenological assumption often employed.<sup>5</sup>

## B. Model BSE

In order to exemplify the results of Ref. [9], which we have reiterated and generalized in Sec. III A, we must have an explicit form for the kernel  $K_{tu}^{rs}(q, k; P)$  in Eq. (25). The form must be such as to preserve the AV WTI, Eq. (28), which requires a truncation of the skeleton expansion for  $K_{tu}^{rs}(q, k; P)$  that is consistent with Eq. (22); our *Ansatz* for the kernel of Eq. (1). The ‘‘ladder truncation’’ fulfills this requirement [12,13]:

$$K_{tu}^{rs}(q, k; P) = -\mathcal{G}((k-q)^2) D_{\nu\nu}^{\text{free}}(k-q) \left( \gamma_\mu \frac{\lambda^a}{2} \right)_{ir} \left( \gamma_\nu \frac{\lambda^a}{2} \right)_{su}, \quad (48)$$

in which case Eq. (25) becomes

<sup>5</sup>In QCD, the integral defining  $r_H$  diverges logarithmically, like the trace of the chiral limit quark propagator (vacuum quark condensate), which is the reason why the right-hand side of Eq. (41) is independent of the renormalization point. This is unlike the trace of the  $\hat{m} \neq 0$  quark propagator, which diverges quadratically.

$$\begin{aligned} & \Gamma_H(k;P) + \int_q^\Lambda \mathcal{G}((k-q)^2) D_{\mu\nu}^{\text{free}}(k-q) \frac{\lambda^a}{2} \gamma_\mu S(q_+) \Gamma_H(q;P) \\ & \times S(q_-) \frac{\lambda^a}{2} \gamma_\nu = 0, \end{aligned} \quad (49)$$

and the normalization condition, Eq. (27), simplifies because the last term vanishes when  $K_{\mu\nu}^{rs}(q,k;P)$  is independent of  $P_\mu$ .

#### IV. NUMERICAL RESULTS

##### A. Solution of the quark DSE

Using Eqs. (1) and (22) our model quark DSE is

$$S(p, \mu)^{-1} = Z_2 i \gamma \cdot p + Z_4 m(\mu) + \Sigma'(p, \Lambda), \quad (50)$$

with the regularized quark self-energy

$$\Sigma'(p, \Lambda) \doteq \int_q^\Lambda \mathcal{G}((p-q)^2) D_{\mu\nu}^{\text{free}}(p-q) \frac{\lambda^a}{2} \gamma_\mu S(q) \frac{\lambda^a}{2} \gamma_\nu, \quad (51)$$

where  $\mathcal{G}(k^2)$  is given in Eq. (23). Equation (50) is a pair of coupled integral equations for the functions  $A(p^2, \mu^2)$  and  $B(p^2, \mu^2)$  defined in Eq. (2).

In the case of explicit chiral symmetry breaking  $\hat{m} \neq 0$ , the renormalization boundary condition of Eq. (3) is straightforward to implement. Writing

$$\Sigma'(p, \Lambda) \doteq i \gamma \cdot p (A'(p^2, \Lambda^2) - 1) + B'(p^2, \Lambda^2), \quad (52)$$

Eq. (3) entails

$$Z_2(\mu^2, \Lambda^2) = 2 - A'(\mu^2, \Lambda^2)$$

and

$$m(\mu) = Z_2(\mu^2, \Lambda^2) m_{\text{bm}}(\Lambda^2) + B'(\mu^2, \Lambda^2) \quad (53)$$

and hence

$$A(p^2, \mu^2) = 1 + A'(p^2, \Lambda^2) - A'(\mu^2, \Lambda^2), \quad (54)$$

$$B(p^2, \mu^2) = m(\mu) + B'(p^2, \Lambda^2) - B'(\mu^2, \Lambda^2). \quad (55)$$

From Sec. II A 1, having fixed the solutions at a single renormalization point  $\mu$ , their form at another point  $\bar{\mu}$  is given by

$$\begin{aligned} S^{-1}(p, \bar{\mu}) &= i \gamma \cdot p A(p^2, \bar{\mu}^2) + B(p^2, \bar{\mu}^2) \\ &= \frac{Z_2(\bar{\mu}^2, \Lambda^2)}{Z_2(\mu^2, \Lambda^2)} S^{-1}(p, \mu). \end{aligned} \quad (56)$$

[Recall that  $M(p^2)$  is independent of the renormalization point.] This feature is manifest in our solutions. It means that, in evolving the renormalization point to  $\bar{\mu}$ , the ‘‘1’’ in Eq. (54) is replaced by  $Z_2(\bar{\mu}^2, \Lambda^2)/Z_2(\mu^2, \Lambda^2)$ , and the

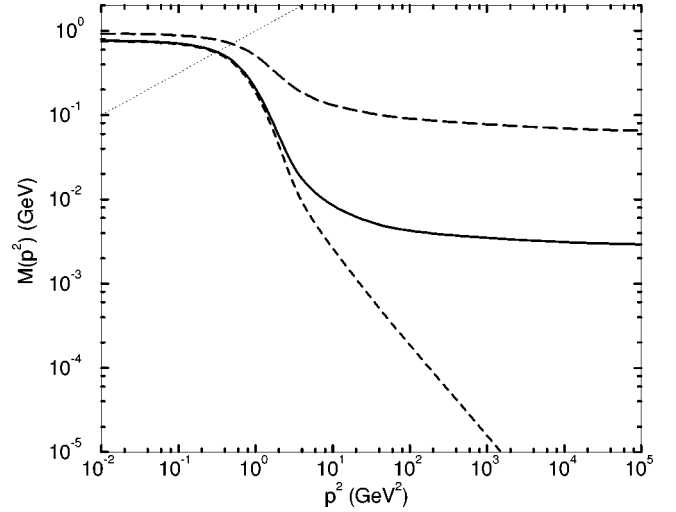


FIG. 2. The renormalized dressed-quark mass function  $M(p^2)$  obtained by solving Eq. (50) using the parameters in Eq. (24):  $u/d$  quark (solid line),  $s$  quark (long-dashed line), and chiral limit (dashed line). The renormalization point is  $\mu = 19$  GeV. The intersection of the line  $M^2(p) = p^2$  (dotted line) with each curve defines the Euclidean constituent-quark mass  $M^E$ .

‘‘ $m(\mu)$ ’’ in Eq. (55) by  $m(\bar{\mu})$ ; i.e., the ‘‘seeds’’ in the integral equation evolve according to the QCD renormalization group.

As also remarked in Sec. II A 1, the chiral limit in QCD is unambiguously defined by  $\hat{m} = 0$ . In this case there is no perturbative contribution to the scalar piece of the quark self-energy,  $B(p^2, \mu^2)$ , and, in fact, there is no scalar, masslike divergence in the perturbative calculation of the self-energy. It follows that  $Z_2(\mu^2, \Lambda^2) m_{\text{bm}}(\Lambda^2) = 0$ ,  $\forall \Lambda$  and, from Eqs. (53) and (55), that there is no subtraction in the equation for  $B(p^2, \mu^2)$ ; i.e., Eq. (55) becomes

$$B(p^2, \mu^2) = B'(p^2, \Lambda^2), \quad (57)$$

with  $\lim_{\Lambda \rightarrow \infty} B'(p^2, \Lambda^2) < \infty$ .<sup>6</sup> In terms of the renormalized current-quark mass the existence of DCSB means that, in the chiral limit,  $M(\mu^2) \sim O(1/\mu^2)$ , up to  $\ln \mu^2$  corrections.

In Fig. 2 we present the renormalized dressed-quark mass function  $M(p^2)$  obtained by solving Eq. (50) using the parameters in Eq. (24) and in the chiral limit. (Recall that  $\mu = 19$  GeV, which is large enough to be in the perturbative domain.)

It is clear from this figure that the light-quark mass function is characterized by a significant infrared enhancement, a direct result of that in the effective coupling,  $\mathcal{G}(k^2)$ . Introducing the Euclidean constituent-quark mass  $M^E$  as the solution of  $p^2 = M^2(p^2)$ , the ratio  $M_f^E/m_f(\mu)$ , where  $f$  labels the quark flavor and  $m_f(\mu)$  is given in Eq. (24), is a single,

<sup>6</sup>This is a model-independent statement; i.e., it is true in any study that preserves at least the one-loop renormalization group behavior of QCD.



indicative, and quantitative measure of the nonperturbative effects of gluon dressing on the quark propagator. We find

|              |          |                        |      |
|--------------|----------|------------------------|------|
|              | $M^E$    | $\frac{M^E}{m_f(\mu)}$ |      |
| chiral limit | 0.55 GeV | $\infty$               | (58) |
| $u/d$        | 0.56     | 150                    |      |
| $s$          | 0.70     | 8.5                    |      |

which clearly indicates the magnitude of this effect for light quarks. The ratio  $M^E/m_f(\mu)$  takes a value of  $O(1)$  for heavy quarks [37] because the current-quark mass is much larger than the mass scale characterizing the infrared enhancement in the effective coupling,  $\Lambda_{\text{QCD}}$ . This means that in the spacelike region the momentum dependence of the heavy-quark mass function is dominated by perturbative effects.<sup>7</sup>

In typical quark model calculations [36] the ‘‘constituent-quark’’ masses are  $M_{u/d}=0.33$  GeV and  $M_s=0.55$  GeV. These are within a factor of 2 of the values in Eq. (58) and are in the ratio  $M_{u/d}/M_s=0.60$ . From Eq. (58) we find  $M_{u/d}^E/M_s^E=0.80$ . The comparison of numerous DSE studies makes it clear that this correspondence between  $M_f$  and  $M_f^E$  is robust. It provides a qualitative understanding of the nature of the ‘‘constituent-quark’’ mass; i.e., it is a quantitative measure of the nonperturbative modification of quark propagation characteristics by gluon dressing. Its magnitude is a signal of the enhancement of the quark-quark interaction in the infrared.

The qualitative difference between the behavior of  $M(p^2)$  in the chiral limit and in the presence of explicit chiral symmetry breaking is manifest in Fig. 2. In the presence of explicit chiral symmetry breaking Eq. (8) describes the form of  $M(p^2)$  for  $p^2 > O(1 \text{ GeV}^2)$ . In the chiral limit, however, the ultraviolet behavior is given by

$$M(p^2) \stackrel{\text{large } p^2}{=} \frac{2\pi^2\gamma_m}{3} \frac{(-\langle \bar{q}q \rangle^0)}{p^2(\frac{1}{2}\ln[p^2/\Lambda_{\text{QCD}}^2])^{1-\gamma_m}}, \quad (59)$$

where  $\langle \bar{q}q \rangle^0$  is the renormalization-point-independent vacuum quark condensate.<sup>8</sup> Analyzing our chiral limit solution we find

$$-\langle \bar{q}q \rangle^0 = (0.227 \text{ GeV})^3. \quad (60)$$

This is a reliable means of determining  $\langle \bar{q}q \rangle^0$  because corrections to Eq. (59) are suppressed by powers of  $\Lambda_{\text{QCD}}^2/\mu^2$ .

Equation (43) defines the renormalization-point-dependent vacuum quark condensate

<sup>7</sup>Quark confinement entails that there is no ‘‘pole mass’’ [35], which would be the solution of  $p^2 + M^2(p^2) = 0$ . Hence, this definition of  $M^E$  is arbitrary; a factor of 2 is certainly unimportant with respect to the qualitative features that this quantity characterizes.

<sup>8</sup>The momentum dependence of this result is characteristic of the QCD renormalization group at one loop [38] and demonstrates that the truncation we employ preserves this feature.

$$\begin{aligned} -\langle \bar{q}q \rangle_\mu^0 \Big|_{\mu=19 \text{ GeV}} &\doteq \left( \lim_{\Lambda \rightarrow \infty} Z_4(\mu, \Lambda) N_c \right. \\ &\times \left. \int_q^\Lambda \text{tr}_{\text{Dirac}}[S_{\hat{m}=0}(q)] \right) \Big|_{\mu=19 \text{ GeV}} \\ &= (0.275 \text{ GeV})^3. \end{aligned} \quad (61)$$

We have established explicitly that  $m(\mu)\langle \bar{q}q \rangle_\mu^0 = \text{const}$ , independent of  $\mu$  with the value depending on the quark flavor, and hence

$$m(\mu)\langle \bar{q}q \rangle_\mu^0 \doteq \hat{m}\langle \bar{q}q \rangle^0, \quad (62)$$

which unambiguously defines the renormalization-point-independent current-quark masses. From this and Eqs. (24), (60), and (61) we extract the values of these masses appropriate to our model:

$$\hat{m}_{u/d} = 6.60 \text{ MeV}, \quad \hat{m}_s = 147 \text{ MeV}. \quad (63)$$

Using Eq. (8) these values yield  $m_{u/d}(\mu) = 3.2$  MeV and  $m_s(\mu) = 72$  MeV, which are within  $\sim 10\%$  of our actual values in Eq. (24). This indicates that higher-loop corrections to the one-loop formulas, which are present in the solution of the integral equation as made evident by  $A(p^2, \mu^2) \neq 1$ , provide contributions of  $< 10\%$  at  $p^2 = \mu^2$ . These contributions decrease with increasing  $p^2$ .<sup>9</sup>

From the renormalization-point-invariant product in Eq. (62) we obtain

$$-\langle \bar{q}q \rangle_\mu^0 \Big|_{\mu=1 \text{ GeV}} \doteq (\ln[1/\Lambda_{\text{QCD}}])^{\gamma_m} \langle \bar{q}q \rangle^0 = (0.241 \text{ GeV})^3. \quad (64)$$

This result can be compared directly with the value of the quark condensate employed in contemporary phenomenological studies [39]:  $(0.236 \pm 0.008 \text{ GeV})^3$ . We note that increasing  $\omega \rightarrow 1.5\omega$  in  $\mathcal{G}(k^2)$  increases the calculated value in Eq. (64) by  $\sim 10\%$ . Obtaining broad agreement with the contemporary phenomenological value of  $\langle \bar{q}q \rangle_\mu^0 \Big|_{\mu=1 \text{ GeV}}$  was a means we employed to constrain the value of this parameter. However, we made no attempt to fine-tune  $\omega$  or thereby our calculated value of  $\langle \bar{q}q \rangle_\mu^0 \Big|_{\mu=1 \text{ GeV}}$ .

In conjunction with Eq. (64) we define  $m_f^{1 \text{ GeV}}$  via Eq. (8) using Eq. (63):

$$m_{u/d}^{1 \text{ GeV}} = 5.5 \text{ MeV}, \quad m_s^{1 \text{ GeV}} = 130 \text{ MeV}. \quad (65)$$

These values differ slightly from those discussed in Sec. II B 2 for the reasons described above. It is now clear, from Eq. (62), that lower values of the current-quark masses, as canvassed in Ref. [30], are admissible in our phenomenological study only via an increase in  $\langle \bar{q}q \rangle_\mu^0 \Big|_{\mu=1 \text{ GeV}}$ .

After this discussion of the vacuum quark condensate it is now straightforward to determine the accuracy of Eqs. (44) and (45). Using experimental values on the left-hand side, we find

<sup>9</sup>Our model for the kernel of the quark DSE is not constructed to preserve the two-loop, perturbative behavior of QCD. Hence a direct comparison at this level is not meaningful.

TABLE I. Calculated values of the properties of light pseudoscalar mesons composed of a quark and antiquark of equal mass. The mass ( $m_\pi^{\text{expt}}=0.1385$ ) and decay constant ( $f_\pi^{\text{expt}}=0.0924$ ) are in GeV, and  $\mathcal{R}_H$  is dimensionless. With the exception of the calculations that retain only the zeroth Chebyshev moment, labeled by “ $U_0$  only,” the results are independent of the momentum partitioning parameter  $\eta_p$ .

| All amplitudes                    | $\pi$   |         |                 | Chiral limit |        |                 | $s\bar{s}$     |                |                 |
|-----------------------------------|---------|---------|-----------------|--------------|--------|-----------------|----------------|----------------|-----------------|
|                                   | $m_\pi$ | $f_\pi$ | $\mathcal{R}_H$ | $m_0$        | $f^0$  | $\mathcal{R}_H$ | $m_{s\bar{s}}$ | $f_{s\bar{s}}$ | $\mathcal{R}_H$ |
| Method (A)                        | 0.1385  | 0.0924  | 1.01            | 0.0          | 0.0898 | 1.00            | 0.685          | 0.129          | 1.00            |
| $U_0$ only                        | 0.136   | 0.0999  | 0.95            | 0.0          | 0.0972 | 0.94            | 0.675          | 0.137          | 0.95            |
| $U_0$ and $U_1$                   | 0.1385  | 0.0925  | 1.00            | 0.0          | 0.0898 | 1.00            | 0.685          | 0.129          | 1.00            |
| <i>E</i> only                     |         |         |                 |              |        |                 |                |                |                 |
| Method (A)                        | 0.105   | 0.0667  | 1.82            | 0.0          | 0.0649 | 1.81            | 0.512          | 0.092          | 1.68            |
| $U_0$ only                        | 0.105   | 0.0667  | 1.82            | 0.0          | 0.0649 | 1.81            | 0.513          | 0.092          | 1.69            |
| <i>E, F</i>                       |         |         |                 |              |        |                 |                |                |                 |
| Method (A)                        | 0.136   | 0.0992  | 0.95            | 0.0          | 0.0965 | 0.95            | 0.677          | 0.137          | 0.95            |
| $U_0$ only                        | 0.136   | 0.0992  | 0.95            | 0.0          | 0.0965 | 0.95            | 0.678          | 0.138          | 0.95            |
| <i>E, F, <math>\hat{G}</math></i> |         |         |                 |              |        |                 |                |                |                 |
| Method (A)                        | 0.140   | 0.0917  | 1.01            | 0.0          | 0.0891 | 1.00            | 0.688          | 0.128          | 1.01            |
| $U_0$ only                        | 0.136   | 0.0992  | 0.95            | 0.0          | 0.0965 | 0.95            | 0.678          | 0.138          | 0.95            |
| $U_0$ and $U_1$                   | 0.140   | 0.0917  | 1.01            | 0.0          | 0.0891 | 1.00            | 0.689          | 0.128          | 1.01            |

$$(0.0924 \times 0.1385)^2 = (0.113 \text{ GeV})^4$$

$$[\text{cf. } (0.111 \text{ GeV})^4 = 2 \times 0.0055 \times 0.24^3], \quad (66)$$

$$(0.113 \times 0.495)^2 = (0.237 \text{ GeV})^4$$

$$[\text{cf. } (0.206 \text{ GeV})^4 = (0.0055 + 0.13) \times 0.24^3], \quad (67)$$

which indicates that  $O(\hat{m}^2)$  corrections begin to become important at current-quark masses near that of the  $s$  quark. We emphasize that we did not use these equations in fitting the current-quark masses but, as described in Sec. IV B, solved the model BSE, Eq. (49), using the dressed-quark propagators obtained as a solution of Eq. (50). In this procedure, changes in  $\langle \bar{q}q \rangle^0$  effected by modifying the model parameters are compensated for by changes in  $\hat{m}_{u/d}$  and  $\hat{m}_s$ . Therefore the comparisons in Eqs. (66) and (67), which involve a product of these quantities, remain meaningful and the conclusion remains valid.<sup>10</sup>

### B. Solution of the BSE

To solve Eq. (49) we modify it by introducing an eigenvalue  $\lambda(P^2)$ ,

$$\begin{aligned} \Gamma_H(k;P) + \lambda(P^2) \int_q^\Lambda \mathcal{G}((k-q)^2) D_{\mu\nu}^{\text{free}}(k-q) \frac{\lambda^a}{2} \gamma_\mu \mathcal{S}(q_+) \\ \times \Gamma_H(q;P) \mathcal{S}(q_-) \frac{\lambda^a}{2} \gamma_\nu = 0, \end{aligned} \quad (68)$$

<sup>10</sup>Using our calculated values of  $f_\pi$ ,  $m_\pi$ ,  $f_K$ , and  $m_K$ , Tables I and II, the only change is in Eq. (67), where  $0.237 \rightarrow 0.233$ .

which yields an equation that has a solution  $\forall P^2$ , characterized by the value of  $\lambda(P^2)$ . The original problem is solved when that  $P^2$  is found for which  $\lambda(P^2) = 1$ , which will occur at  $P^2 < 0$  in our metric.

For  $P^2 = -\mathcal{P}^2 < 0$ , solving Eq. (68) requires the dressed-quark propagator  $\mathcal{S}(q_+)$  on the parabola,  $4\eta_p^2 \mathcal{P}^2 \text{Re}(q_+^2) = \text{Im}(q_+^2)^2 - 4(\eta_p^2 \mathcal{P}^2)^2$ , in the complex- $q_+^2$  plane, and  $\mathcal{S}(q_-)$  on the parabola,  $4(1-\eta_p)^2 \mathcal{P}^2 \text{Re}(q_-^2) = \text{Im}(q_-^2)^2 - 4[(1-\eta_p)^2 \mathcal{P}^2]^2$ , in the complex- $q_-^2$  plane. For complex arguments in the dressed-quark propagator the quark DSE requires the effective coupling at complex values of its argument. Equation (68), however, still only requires  $\mathcal{G}(k^2)$  on the real  $k^2 > 0$  axis. The specification of  $\mathcal{G}(k^2)$  is the primary element in the definition of the model and our *Ansatz* is motivated by studies that are restricted to real  $k^2 > 0$ . In employing this *Ansatz* at complex values of its arguments we are exploring an unconstrained domain. Solving numerically for  $\mathcal{S}(p)$  in the complex- $p^2$  plane is straightforward. However, complex-conjugate branch points in the (confining) solution introduce numerical complications in solving the BSE for bound states containing a single heavy constituent.<sup>11</sup>

The general form of the solution of the BSE, Eq. (49), is given in Eq. (26) where the scalar functions depend on the variables  $k^2$  and  $k \cdot P$ , and are labeled by the eigenvalue  $P^2$ . From this it is clear that the integrand in Eq. (68) depends on

<sup>11</sup>This branch-point pair is present because of the infrared enhancement in our *Ansatz* for the effective coupling but may be an artifact of the rainbow approximation, Eq. (21). Reference [22] demonstrates that dressing the vertex, consistent with the constraints of Refs. [20], can significantly affect the analytic properties of  $\mathcal{S}(p)$  while maintaining the essence of quark confinement [35], i.e., that  $\mathcal{S}(p)$  not have a Lehmann representation.

TABLE II. Calculated properties of the  $K$  meson for various values of the momentum partitioning parameter  $\eta_P$ ; “-” means that no bound state solution exists in this case. The mass ( $m_K^{\text{expt}}=0.496$ ) and decay constant ( $f_K^{\text{expt}}=0.113$ ) are in GeV, and  $\mathcal{R}_K$  is dimensionless.

| All amplitudes                    | $\eta_P=0.50$ |       |                 | $\eta_P=0.25$ |       |                 | $\eta_P=0.00$ |       |                 |
|-----------------------------------|---------------|-------|-----------------|---------------|-------|-----------------|---------------|-------|-----------------|
|                                   | $m_K$         | $f_K$ | $\mathcal{R}_K$ | $m_K$         | $f_K$ | $\mathcal{R}_K$ | $m_K$         | $f_K$ | $\mathcal{R}_K$ |
| Method (A)                        | 0.497         | 0.109 | 1.01            | 0.497         | 0.109 | 1.01            | 0.497         | 0.109 | 1.01            |
| $U_0$ only                        | 0.469         | 0.117 | 0.96            | 0.482         | 0.117 | 0.95            | 0.475         | 0.113 | 1.02            |
| $U_0$ and $U_1$                   | 0.500         | 0.111 | 1.00            | 0.497         | 0.109 | 1.01            | 0.498         | 0.110 | 1.00            |
| $U_0, U_1,$ and $U_2$             | 0.497         | 0.109 | 1.01            | 0.497         | 0.109 | 1.01            | 0.496         | 0.109 | 1.01            |
| <i>E</i> only                     |               |       |                 |               |       |                 |               |       |                 |
| Method (A)                        | 0.430         | 0.079 | 1.55            | 0.430         | 0.079 | 1.55            | 0.429         | 0.076 | 1.55            |
| $U_0$ only                        | 0.380         | 0.077 | 1.54            | 0.401         | 0.076 | 1.51            | 0.415         | 0.073 | 1.55            |
| $U_0$ and $U_1$                   | 0.439         | 0.089 | 1.52            | 0.430         | 0.078 | 1.55            | 0.431         | 0.076 | 1.57            |
| $U_0, U_1,$ and $U_2$             | 0.430         | 0.078 | 1.55            | 0.430         | 0.078 | 1.55            | 0.427         | 0.076 | 1.55            |
| <i>E, F</i>                       |               |       |                 |               |       |                 |               |       |                 |
| Method (A)                        | 0.587         | 0.17  | 0.79            | 0.557         | 0.14  | 0.86            | 0.533         | 0.11  | 0.94            |
| $U_0$ only                        | 0.505         | 0.12  | 0.82            | 0.518         | 0.11  | 0.86            | 0.512         | 0.11  | 0.96            |
| $U_0$ and $U_1$                   | -             | -     | -               | 0.556         | 0.14  | 0.86            | 0.537         | 0.12  | 0.94            |
| $U_0, U_1,$ and $U_2$             | 0.583         | 0.16  | 0.79            | 0.557         | 0.14  | 0.86            | 0.532         | 0.12  | 0.93            |
| <i>E, F, <math>\hat{G}</math></i> |               |       |                 |               |       |                 |               |       |                 |
| Method (A)                        | 0.500         | 0.108 | 1.01            | 0.500         | 0.108 | 1.01            | 0.500         | 0.108 | 1.01            |
| $U_0$ only                        | 0.471         | 0.116 | 0.96            | 0.484         | 0.116 | 0.95            | 0.477         | 0.112 | 1.02            |
| $U_0$ and $U_1$                   | 0.504         | 0.110 | 1.00            | 0.500         | 0.108 | 1.01            | 0.502         | 0.109 | 1.00            |
| $U_0, U_1,$ and $U_2$             | 0.500         | 0.108 | 1.01            | 0.500         | 0.108 | 1.01            | 0.499         | 0.108 | 1.01            |

the scalars  $k^2$ ,  $k \cdot q$ ,  $q^2$ ,  $q \cdot P$ , and  $P^2$ , which takes a fixed value at the solution; i.e., at each value of  $P^2$  the kernel is a function of four independent variables. Solving Eq. (68) can therefore require large-scale computing resources, especially since there are four independent scalar functions in the general form of the solution.

We employed two different techniques in solving Eq. (68). In our primary procedure (A), we treated the scalar functions directly as dependent on two independent variables  $E(k^2, k \cdot P; P^2)$ , etc., which requires straightforward, multidimensional integration at every iteration. Storing the multidimensional kernel requires a large amount of computer memory but the iteration proceeds quickly.

As an adjunct, and because we wish to elucidate qualitative and quantitative effects related to the  $k \cdot P$  dependence of the scalar functions in the BSA, we employed a Chebyshev decomposition procedure (B). To implement this we write

$$E(k^2, k \cdot P; P^2) \approx \sum_{i=0}^{N_{\max}} {}^i E(k^2; P^2) U_i(\cos \beta), \quad (69)$$

with similar expansions for  $F$ ,  $\hat{G} \doteq k \cdot P G$ , and  $H$ , where  $k \cdot P \doteq \cos \beta \sqrt{k^2 P^2}$  and  $\{U_i(x); i=0, \dots, \infty\}$  are Chebyshev polynomials of the second kind orthonormalized according to

$$\frac{2}{\pi} \int_{-1}^1 dx \sqrt{1-x^2} U_i(x) U_j(x) = \delta_{ij}. \quad (70)$$

Substituting this expansion into Eq. (68) allows all but one of the integrals to be evaluated before beginning the iteration. One then solves for the Chebyshev moments  ${}^i E(k^2; P^2)$ . This procedure requires a large amount of time to set up the kernel but does not require large amounts of computer memory.<sup>12</sup>

In order to fit the parameter  $D$  in  $\mathcal{G}(k^2)$  and the current-quark mass  $m_{u/d}(\mu)$  we (1) chose values for these parameters; (2) solved the quark DSE for  $S_{u/d}(p)$ ; (3) used  $\mathcal{G}(k^2)$  and the calculated form of  $S_{u/d}(p)$  to solve the pion BSE for the mass and BSA,  $\Gamma_\pi(k; P)$ , using procedure (A); and (4) used the calculated forms of  $S_{u/d}(p)$  and  $\Gamma_\pi(k; P)$  to calculate  $f_\pi$  from Eq. (33). We repeated this procedure until satisfactory values of  $m_\pi$  and  $f_\pi$  were obtained. Having thus fixed  $D$  we repeated the steps for the  $K$  meson, varying  $m_s(\mu)$  only, in order to obtain the best possible values of  $m_K$  and  $f_K$ . This led to the parameter values quoted in Eq. (24) and the results listed in row one of Tables I and II. This does not represent an exhaustive search of the available parameter space but is sufficient for our purposes.

### C. Discussion of the BSE solution

From Tables I and II, and Eqs. (24), (46), (47), and (64), it is straightforward to calculate

<sup>12</sup>Equation (69) is only an identity in the limit  $N_{\max} \rightarrow \infty$  but, in the present example, an accurate representation of the solution is obtained with  $N_{\max}=1$  or 2, which is consistent with the observations of Ref. [5].

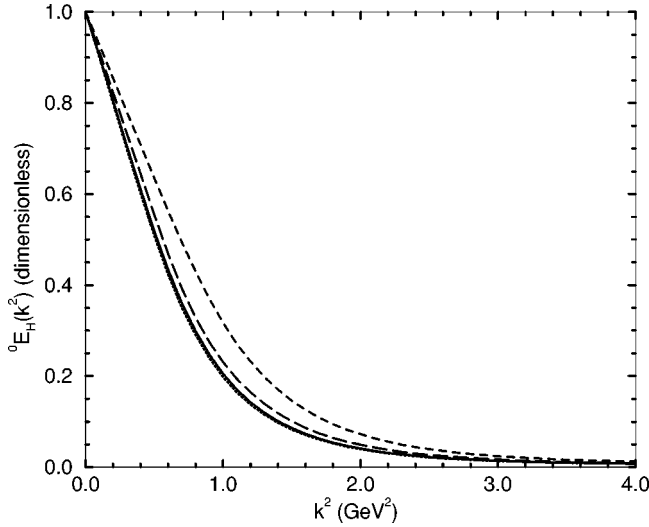


FIG. 3. The zeroth Chebyshev moment of  $E_H(k;P)$ : chiral limit (dotted line),  $\pi$  meson (solid line),  $K$  meson (long-dashed line), and fictitious,  $s\bar{s}$  bound state (dashed line).  $\eta_P = \frac{1}{2}$  in each case. For ease of comparison the BSA's are all rescaled so that  ${}^0E_H(k^2=0) = 1$ .

$$\begin{array}{ccc} -\langle \bar{q}q \rangle_{\mu=1 \text{ GeV}}^{\pi} & -\langle \bar{q}q \rangle_{\mu=1 \text{ GeV}}^K & -\langle \bar{q}q \rangle_{\mu=1 \text{ GeV}}^{s\bar{s}} \\ (0.245 \text{ GeV})^3 & (0.284 \text{ GeV})^3 & (0.317 \text{ GeV})^3 \end{array} \quad (71)$$

showing that, for light pseudoscalars, the ‘‘in-meson condensate’’ that we have defined increases with increasing bound state mass, as does the leptonic decay constant  $f_H$ .<sup>13</sup>

In Tables I and II we list values of the dimensionless ratio

$$\mathcal{R}_H \doteq -\frac{\langle \bar{q}q \rangle_{\mu}^H \mathcal{M}_H}{f_H^2 m_H^2}. \quad (72)$$

A value of  $\mathcal{R}_H = 1$  means that Eq. (41) is satisfied and hence so is the AV WTI.<sup>14</sup> Looking at the tabulated values of  $\mathcal{R}_H$  it is clear that the scalar function  $H$  is not quantitatively important, with the AV WTI being satisfied numerically with the retention of  $E$ ,  $F$ , and  $G$  in the pseudoscalar meson BSA. The values of  $\mathcal{R}_H$ , and the other tabulated quantities, highlight the importance of  $F$  and  $\hat{G}$ :  $F$  is the most important of these functions but  $\hat{G}$  nevertheless provides a significant contribution, particularly for bound states of unequal-mass constituents. We note that a poor value of  $f_H$  is tied to a poor value of  $\mathcal{R}_H$ , which emphasizes the importance of preserving the AV WTI and hence Eq. (38). We have checked explicitly that our complete solutions satisfy Eq. (38).

The tables illustrate the rapid convergence of the Chebyshev decomposition procedure (B), with accurate solutions

<sup>13</sup> $-\langle \bar{q}q \rangle_{\mu}^H / f_H$  is the residue of the bound state pole in the pseudoscalar vertex, just as  $f_H$  is the residue of the bound state pole in the axial-vector vertex. As expected,  $\langle \bar{q}q \rangle_{\mu=1 \text{ GeV}}^{\pi} \approx \langle \bar{q}q \rangle_{\mu=1 \text{ GeV}}^0$ .

<sup>14</sup>It illustrates that the pseudoscalar-meson pole in the axial-vector vertex is related to the pseudoscalar-meson pole in the pseudoscalar vertex in the manner we have elucidated. A finite value in the chiral limit emphasizes that  $m_H^2 \propto \mathcal{M}_H$  as  $\mathcal{M}_H \rightarrow 0$ .

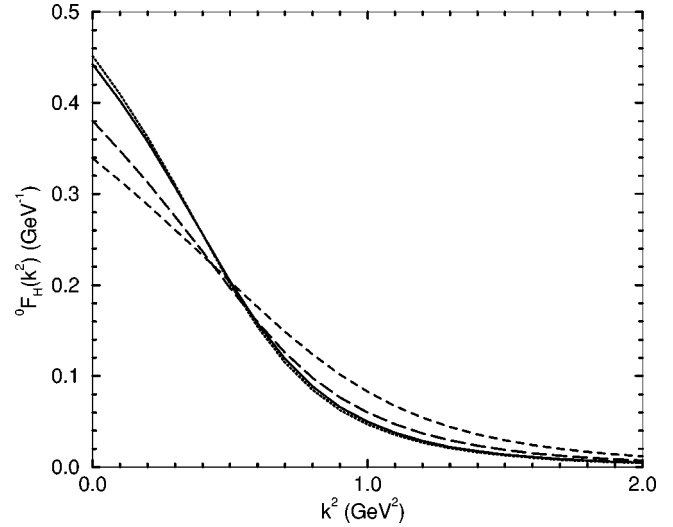


FIG. 4. The zeroth Chebyshev moment of  $F_H(k;P)$ : chiral limit (dotted line),  $\pi$  meson (solid line),  $K$  meson (long-dashed line), and fictitious,  $s\bar{s}$  bound state (dashed line).  $\eta_P = \frac{1}{2}$  in each case. For ease of comparison the BSA's are all rescaled so that  ${}^0F_H(k^2=0) = 1$ .

being obtained with the zeroth and first moments for bound states of equal-mass constituents.<sup>15</sup> The same is true for bound states of unequal-mass constituents *provided* all Dirac amplitudes are retained in the solution.

One observes that when the  $k \cdot P$  dependence of the scalar functions in the meson Bethe-Salpeter amplitude is included, physical observables are *independent* of the momentum partitioning parameter  $\eta_P$ . These calculations elucidate the manner in which this necessary requirement in covariant bound state studies is realized: The bound state amplitude depends on  $\eta_P$  in just that fashion which ensures physical quantities do not. All the scalar functions in the BSA must be included to ensure this.

The tables also illustrate clearly the effect of the current-quark mass via a comparison of the chiral limit pion with the physical pion, the kaon, and a fictitious, pseudoscalar,  $s\bar{s}$  bound state. One observes that  $f_H$  is weakly sensitive to increasing the current-quark mass; for example, we obtain  $f^0/f_{\pi} = 0.97$ , which is consistent with expectations based on effective chiral Lagrangians. However,  $m_H^2$  rises quickly, before becoming sensitive to effects nonlinear in the current-quark mass.<sup>16</sup>

<sup>15</sup>We note that for equal-mass constituents  $\hat{G} = k \cdot P G$  is an odd function of  $k \cdot P$  and hence  ${}^0\hat{G} = 0$ . Therefore it first contributes at  $O(U_1)$ .

<sup>16</sup>We note that our calculated value of  $m_{s\bar{s}}$  is within 3% of that obtained for this fictitious bound state in Ref. [6]. However, the results in Ref. [6] depend on  $\eta_P$ , which is an artifact of the solution procedure adopted therein. In that study a derivative-expansion and extrapolation procedure was employed in order to avoid a direct solution for the quark propagator functions  $A(p^2)$  and  $B(p^2)$  at complex values of their arguments. In addition, in most instances only the zeroth Chebyshev moment was retained in the Chebyshev expansion of the scalar functions in the Bethe-Salpeter wave function:  $\chi_H(q;P) \doteq S(q_+) \Gamma_H(q;P) S(q_-)$ .

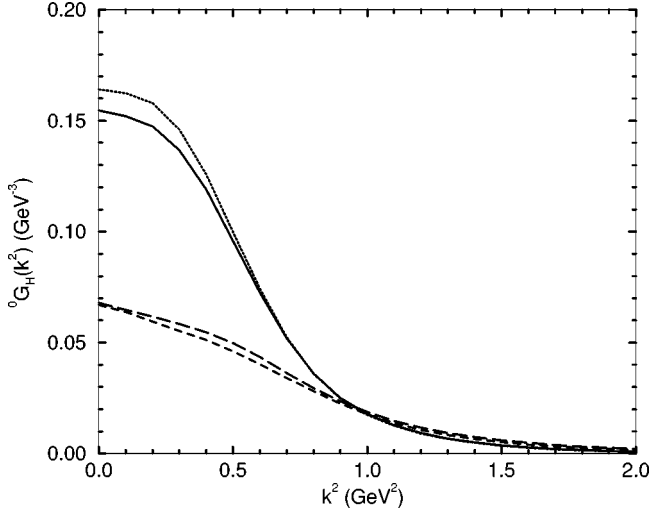


FIG. 5. The zeroth Chebyshev moment of  $G_H(k;P)$ : chiral limit (dotted line),  $\pi$  meson (solid line), fictitious,  $s\bar{s}$  bound state (dashed line), and of  $\hat{G}_H(k;P)$  ( $\text{GeV}^{-1}$ ) for the  $K$  meson (long-dashed line).  $\eta_p = \frac{1}{2}$  in each case. For ease of comparison the BSA's are all rescaled so that  ${}^0E_H(k^2=0)=1$ .

We present the scalar functions in the BSA obtained as solutions of Eq. (49) in Figs. 3–7, focusing on the zeroth Chebyshev moment of each function, which is obtained via

$${}^0E_H(k^2) \doteq \frac{2}{\pi} \int_0^\pi d\beta \sin^2\beta U_0(\cos\beta) E_H(k^2, k \cdot P; P^2), \quad (73)$$

and similarly for  $F$ ,  $G$  ( $\hat{G}$  for the  $K$  meson), and  $H$ . Figure 3 illustrates that the momentum-space width of  ${}^0E_H(k^2)$  increases as the current-quark mass of the bound state constituents increases; Fig. 4, that  ${}^0F_H(k^2=0)$  decreases with increasing current-quark mass but that  ${}^0F_H(k^2)$  is still larger at  $k^2 > 0.5 \text{ GeV}^2$  for bound states of higher mass; Fig. 5, that

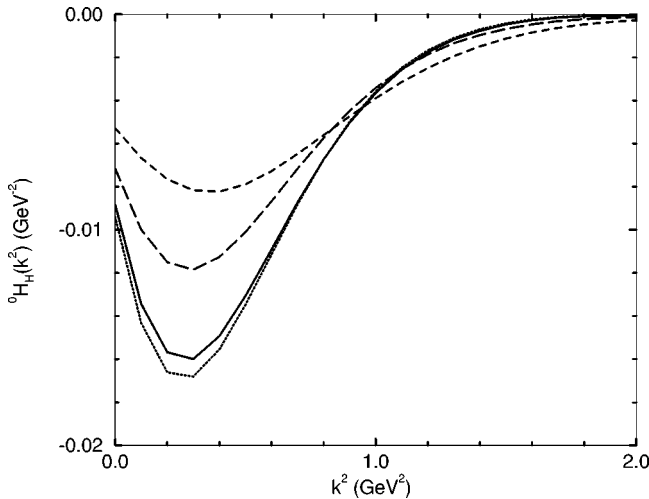


FIG. 6. The zeroth Chebyshev moment of  $H_H(k;P)$ : chiral limit (dotted line),  $\pi$  meson (solid line),  $K$  meson (long-dashed line), and fictitious,  $s\bar{s}$  bound state (dashed line).  $\eta_p = \frac{1}{2}$  in each case. For ease of comparison the BSA's are all rescaled so that  ${}^0E_H(k^2=0)=1$ .

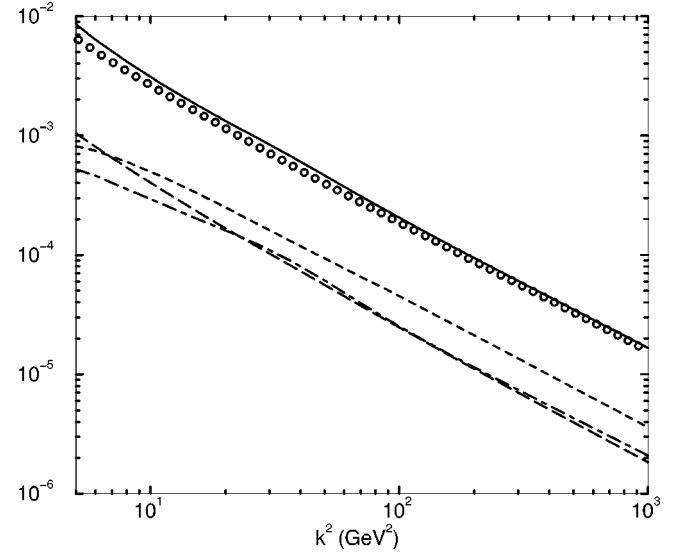


FIG. 7. The asymptotic behavior of the zeroth Chebyshev moments of the functions in the  $\pi$ -meson BSA:  $f_\pi^0 E_\pi(k^2)$  ( $\text{GeV}$ , solid line),  $f_\pi^0 F_\pi(k^2)$  (dimensionless, long-dashed line),  $k^2 f_\pi^0 G_\pi(k^2)$  (dimensionless, dashed line), and  $k^2 f_\pi^0 H_\pi(k^2)$  ( $\text{GeV}$ , dot-dashed line). The momentum dependence is identical to that of the chiral-limit quark mass function  $M(p^2)$ , Eq. (59) ( $\text{GeV}$ , circles). For other pseudoscalar mesons the momentum dependence of these functions is qualitatively the same, although the normalizing magnitude differs.

${}^0G_H(k^2)$  [ ${}^0\hat{G}_K(k^2)$ ] behaves similarly; and Fig. 6, that the same is true for  $H_H(k;P)$  and that it is uniformly small in magnitude thereby explaining its quantitative insignificance. Where comparison is possible, these observations agree qualitatively with Refs. [6,11].

In Fig. 7 we illustrate the large- $k^2$  behavior of the scalar functions in the pseudoscalar BSA. The momentum dependence of  ${}^0E_H(k^2)$  at large  $k^2$  is identical to that of the chiral-limit quark mass function  $M(p^2)$  in Eq. (59) [40], and characterizes the form of the quark-quark interaction in the ultraviolet. Figure 7 elucidates that this is also true of  ${}^0F_H(k^2)$ ,  $k^2 {}^0G_H(k^2)$  [ $k^2 {}^0\hat{G}_K(k^2)$  for the  $K$  meson], and  $k^2 {}^0H_H(k^2)$ . Each of these functions reaches its ultraviolet limit by  $k^2 \approx 10 \text{ GeV}^2$ , which is very much less than the renormalization point,  $\mu^2 = 361 \text{ GeV}^2$ .

In order to verify Eqs. (34)–(37) it is necessary to consider the inhomogeneous axial-vector vertex equation, Eq. (29), in our truncation of the DSE's, which is

$$\Gamma_{5\mu}^H(k;P) = Z_2 \gamma_5 \gamma_\mu \frac{T^H}{2} - \int_q^\Lambda \mathcal{G}((k-q)^2) D_{\mu\nu}^{\text{free}}(k-q) \frac{\lambda^a}{2} \gamma_\mu \times \mathcal{S}(q_+) \Gamma_{5\mu}^H(q;P) \mathcal{S}(q_-) \frac{\lambda^a}{2} \gamma_\nu. \quad (74)$$

From the homogeneous BSE one already has the equations satisfied by  $E_H(k;0)$ ,  $F_H(k;0)$ ,  $G_H(k;0)$ , and  $H_H(k;0)$ . To proceed, one substitutes Eq. (32) for  $\Gamma_{5\mu}^H(k;P)$  in Eq. (74).

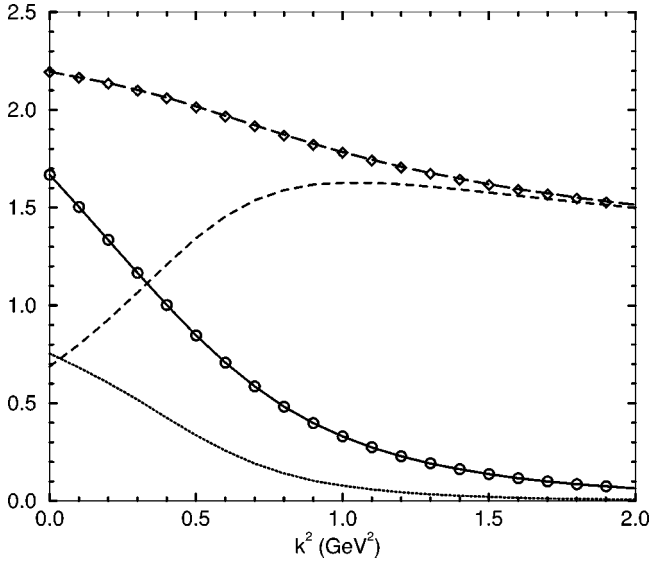


FIG. 8. An illustration of the realisation in our model of the identities Eqs. (34) and (35), which are a necessary consequence of preserving the axial-vector Ward-Takahashi identity. We plot  $f^0 E_H(k;0)$  (GeV, solid line),  $F_R(k;0)$  (dimensionless, dashed line),  $f^0 F_H(k;0)$  (dimensionless, dotted line), and  $F_R(k;0) + 2f_H F_H(k;0)$  (long-dashed line). In each curve the plotted points represent the right-hand side of these equations as obtained in the solution of the chiral-limit quark DSE:  $B(k^2)$  (GeV, circles) and  $A(k^2)$  (dimensionless, diamonds).

Using the coupled equations for  $E_H(k;0)$ , etc., one can identify and eliminate each of the pole terms associated with pseudoscalar bound state. (It is the fact that the homogeneous BSE is linear in the BSA that allows this.) This yields a system of coupled equations for  $F_R(k;0)$ ,  $G_R(k;0)$ , and  $H_R(k;0)$ , which can be solved without complication. [The factor of  $Z_2$  automatically ensures that  $F_R(k^2 = \mu^2; P=0) = 1$ .] We illustrate the realization of the first two identities, Eqs. (34) and (35), in Fig. 8. The remaining two identities, Eqs. (36) and (37), are realized in a similar fashion.

## V. SUMMARY AND CONCLUSION

With renormalization considered explicitly, we have studied the Dyson-Schwinger equation for the dressed-quark propagator  $S(p)$ ; the homogeneous, pseudoscalar meson Bethe-Salpeter equation, which provides the meson's Bethe-Salpeter amplitude  $\Gamma(k;P)$ , with  $P$  the total momentum of the bound state; and the inhomogeneous BSE's for the fully amputated axial-vector and pseudoscalar vertices  $\Gamma_{5,\mu}(k;P)$  and  $\Gamma_5(k;P)$ , respectively. Independent of assumptions about the form of the quark-quark scattering kernel  $K(q,k;P)$ , we have elucidated the manner in which the axial-vector Ward-Takahashi identity correlates these Schwinger functions and provides important and phenomenologically useful constraints.

We demonstrated that the axial-vector vertex contains a pseudoscalar, bound state pole contribution whose residue is the meson's leptonic decay constant, Eq. (33). The pseudoscalar vertex also contains such a pole term but in this case the residue is related to an "in-meson" quark condensate, Eq. (42), which is equal to the vacuum quark condensate in

the chiral limit, Eq. (43). The AV WTI necessarily entails an identity between these residues, Eq. (41), which is valid *independent* of the current-quark mass of the bound state constituents. The expression commonly known as the Gell-Mann–Oakes–Renner relation is a corollary of this identity. The AV WTI also places constraints on the form of the pseudoscalar meson Bethe-Salpeter amplitude, which necessarily involves quantitatively important terms proportional to  $\gamma_5 \gamma \cdot P$  and  $\gamma \cdot k k \cdot P$  that have hitherto been neglected in phenomenological studies of spectra, and production and scattering processes in QCD. In the chiral limit these constraints take a very simple form: Eqs. (34)–(37).

In Sec. IV B 1 we illustrated these identities and constraints in numerical studies using a rainbow-ladder truncation for  $K(q,k;P)$  motivated by the Abelian approximation, Secs. II B and III B, and defined by an *Ansatz* for the dressed-quark-quark interaction, Fig. 1. The model thus defined preserves the one-loop renormalization-group behavior of QCD, as is clear in our numerical solutions. This aspect of our study facilitated an elucidation of the dominant, ultraviolet (large- $k^2$ ) behavior of the scalar functions in the pseudoscalar meson BSA, Fig. 7. Employing these results in a calculation of the electromagnetic pion form factor yields  $Q^2 F_\pi(Q^2) = \text{const}$ , up to  $\ln Q^2$  corrections, a direct consequence of the model-independent result  ${}^0 F_H(k^2) \sim k^2 {}^0 \hat{G}_K(k^2) \sim 1/[\ln(k/\Lambda_{\text{QCD}})]^{1-\gamma_m}$  [41]. The pseudoscalar amplitude  $E_\pi(k;P)$  does not contribute to the asymptotic form of  $F_\pi(Q^2)$ .<sup>17</sup>

In the course of these numerical studies we explored the feasibility of two methods for solving the homogeneous Bethe-Salpeter equation with dressed-quark propagators, determined numerically, and without a three-dimensional reduction: (A) treating the problem directly as a multidimensional integral equation, or (B) employing a Chebyshev expansion of the scalar functions in the BSA in order to obtain a system of one-dimensional integral equations. We favored (A) because it provides a simpler numerical procedure, the program runs quickly, and computer memory usage was not a consideration. Nevertheless, we observed that the Chebyshev expansion converged quickly, with at most two moments being necessary to reproduce the solution obtained using (A), Sec. IV B 1. Importantly, we saw that retaining the  $k \cdot P$  dependence of the scalar functions in the meson BSA is all that is necessary to ensure that physical observables are independent of the momentum partitioning parameter that appears in the definition of the relative momentum, which is arbitrary in covariant studies.

We have demonstrated that the Goldstone-boson character

<sup>17</sup>We note that the calculation of the elastic pion form factor involves two pion Bethe-Salpeter amplitudes, which is qualitatively different to the electroproduction studies of Ref. [3], which involve only one meson Bethe-Salpeter amplitude. We therefore expect that the conclusions of Ref. [3] will not be qualitatively sensitive to the omission of all vector meson Dirac amplitudes other than  $\gamma_\mu$  since, in that calculation, the Bethe-Salpeter amplitude acts only to restrict the support of the integrand and the asymptotic behavior of the cross sections is determined by the behavior of the quark propagator.

of flavor-nonsinglet, pseudoscalar mesons is no impediment to their description as bound states in QCD. It is only important that, in developing the bound state equations, the axial-vector Ward-Takahashi identity be preserved explicitly. This identity necessarily entails relations between the  $n$ -point Schwinger functions (propagators and vertices) relevant to the bound state equation, relations which provide for the manifestation of Goldstone's theorem. In taking account of this, one can in principle construct a single kernel for the Bethe-Salpeter equation that will provide a uniformly good qualitative and quantitative description of the properties of all mesons.

## ACKNOWLEDGMENTS

We acknowledge useful conversations and correspondence with A. Bender, M. C. Birse, F. T. Hawes, J. A. McGovern, P. C. Tandy, and A. G. Williams. C.D.R. is grateful to the Department of Physics and Mathematical Physics at the University of Adelaide for their hospitality and support during a term as a Distinguished Visiting Scholar in which some of this work was conducted. This work was funded by the U.S. Department of Energy, Nuclear Physics Division, under Contract No. W-31-109-ENG-38, and benefited from the resources of the National Energy Research Scientific Computing Center.

- 
- [1] C. D. Roberts and A. G. Williams, *Prog. Part. Nucl. Phys.* **33**, 477 (1994).
- [2] P. C. Tandy, *Prog. Part. Nucl. Phys.* **39**, 117 (1997).
- [3] M. A. Pichowsky and T. -S. H. Lee, *Phys. Rev. D* **56**, 1644 (1997).
- [4] See, for example, R. M. Woloshyn and A. D. Jackson, *Nucl. Phys.* **B64**, 269 (1973); K. Kusaka and A. G. Williams, *Phys. Rev. D* **51**, 7026 (1995); Ref. [5].
- [5] T. Nieuwenhuis and J. A. Tjon, *Few-Body Syst.* **21**, 167 (1996).
- [6] P. Jain and H. J. Munczek, *Phys. Rev. D* **48**, 5403 (1993).
- [7] P. C. Tiemeijer and J. A. Tjon, *Phys. Rev. C* **49**, 494 (1994).
- [8] A. J. Sommerer, J. R. Spence, and J. P. Vary, *Phys. Rev. C* **49**, 513 (1994).
- [9] P. Maris, C. D. Roberts, and P. C. Tandy, "Pion mass and decay constant," e-print nucl-th/9707003.
- [10] F. Gross and J. Milana, *Phys. Rev. D* **50**, 3332 (1994).
- [11] C. J. Burden *et al.*, *Phys. Rev. C* **55**, 2649 (1997).
- [12] A. Bender, C. D. Roberts, and L. v. Smekal, *Phys. Lett. B* **380**, 7 (1996).
- [13] C. D. Roberts, in *Quark Confinement and the Hadron Spectrum II*, edited by N. Brambilla and G. M. Prosperi (World Scientific, Singapore, 1997), pp. 224–230.
- [14] J. Kogut and L. Susskind, *Phys. Rev. D* **10**, 3468 (1974).
- [15] For a heuristic discussion of renormalization in the context of QCD see P. Pascual and R. Tarrach, *QCD: Renormalisation for the Practitioner* (Springer-Verlag, Berlin, 1984).
- [16] M. R. Frank and C. D. Roberts, *Phys. Rev. C* **53**, 390 (1996).
- [17] F. T. Hawes, T. Sizer, and A. G. Williams, *Phys. Rev. D* **55**, 3866 (1997).
- [18] J. S. Ball and T.-W. Chiu, *Phys. Rev. D* **22**, 2542 (1980).
- [19] See also S. K. Kim and M. Baker, *Nucl. Phys.* **B164**, 152 (1980); J. S. Ball and T.-W. Chiu, *Phys. Rev. D* **22**, 2550 (1980).
- [20] A. Bashir, A. Kizilersu, and M. R. Pennington, "The nonperturbative three point vertex in massless quenched QED and perturbation theory constraints," e-print hep-ph/9707421.
- [21] A. G. Williams, G. Krein, and C. D. Roberts, *Ann. Phys. (N.Y.)* **210**, 464 (1991).
- [22] C. J. Burden, C. D. Roberts, and A. G. Williams, *Phys. Lett. B* **285**, 347 (1992).
- [23] F. T. Hawes, C. D. Roberts, and A. G. Williams, *Phys. Rev. D* **49**, 4683 (1994).
- [24] See, for example, D. Atkinson and P. W. Johnson, *Phys. Rev. D* **37**, 2296 (1988).
- [25] D. C. Curtis and M. R. Pennington, *Phys. Rev. D* **42**, 4165 (1990).
- [26] F. T. Hawes (private communication).
- [27] M. R. Pennington, "Calculating hadronic properties in strong QCD," e-print hep-ph/9611242.
- [28] N. Brown and M. R. Pennington, *Phys. Rev. D* **39**, 2723 (1989).
- [29] H. J. Munczek and A. M. Nemirovsky, *Phys. Rev. D* **28**, 181 (1983).
- [30] T. Bhattacharya, R. Gupta, and K. Maltman, "Duality and the extraction of light quark masses from finite energy and QCD sum rules," e-print hep-ph/9703455.
- [31] N. Brambilla and A. Vairo, *Phys. Rev. D* **56**, 1445 (1997).
- [32] C. H. Llewellyn-Smith, *Ann. Phys. (N.Y.)* **53**, 521 (1969).
- [33] G. Preparata and W. I. Weisberger, *Phys. Rev. D* **175**, 1965 (1968).
- [34] D. W. McKay, H. J. Munczek, and B.-L. Young, *Phys. Rev. D* **37**, 195 (1988).
- [35] See, for example, C. D. Roberts, A. G. Williams, and G. Krein, *Int. J. Mod. Phys. A* **4**, 1681 (1992); Ref. [23]; Sec. (6.2) of Ref. [1]; and P. Maris, *Phys. Rev. D* **52**, 6087 (1995).
- [36] For example, S. Capstick and B. D. Keister, "Baryon magnetic moments in a relativistic quark model," e-print nucl-th/9611055.
- [37] M. A. Ivanov *et al.*, "Semileptonic decays of heavy mesons," e-print nucl-th/9704039 [*Phys. Lett. B* (to be published)].
- [38] K. Lane, *Phys. Rev. D* **10**, 2605 (1976); H. D. Politzer, *Nucl. Phys.* **B117**, 397 (1976).
- [39] D. B. Leinweber, *Ann. Phys. (N.Y.)* **254**, 328 (1997).
- [40] V. Miransky, *Mod. Phys. Lett. A* **5**, 1979 (1990).
- [41] C. D. Roberts, "Confinement and Hadron Form Factors," presented at the Bonn Workshop on Confinement Physics, Bonn, Germany, 1997; P. Maris, "Mesons as Bound States," presented at the Eighth International Workshop on Light-Cone QCD and Nonperturbative Hadronic Physics, Lutsen, Minnesota, 1997: <http://www.d.umn.edu/physics/program.htm>; P. Maris and C. D. Roberts (unpublished).